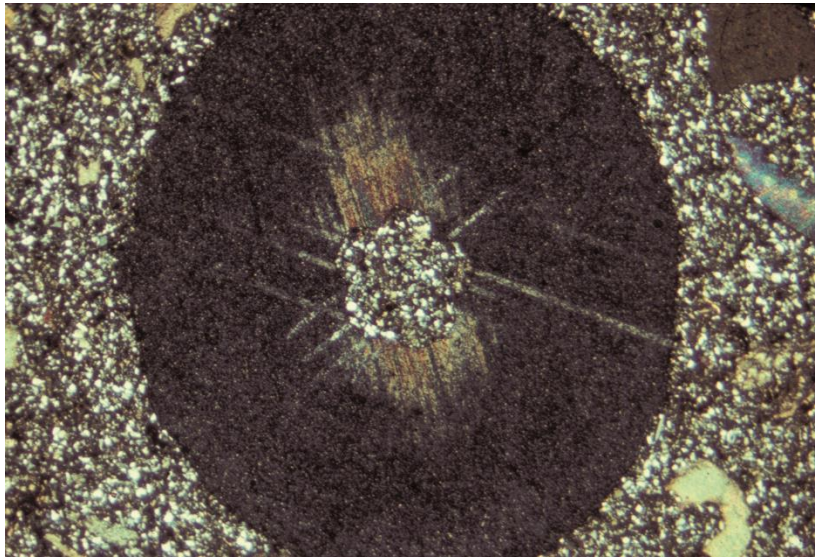

The Three Elements of Structural Geology

Sponsored by

Third Sessions

(Part 5)

ExxonMobil

Terry Engelder

Professor of Geosciences, The Pennsylvania State University

AAPG Africa Region

Table of Contents

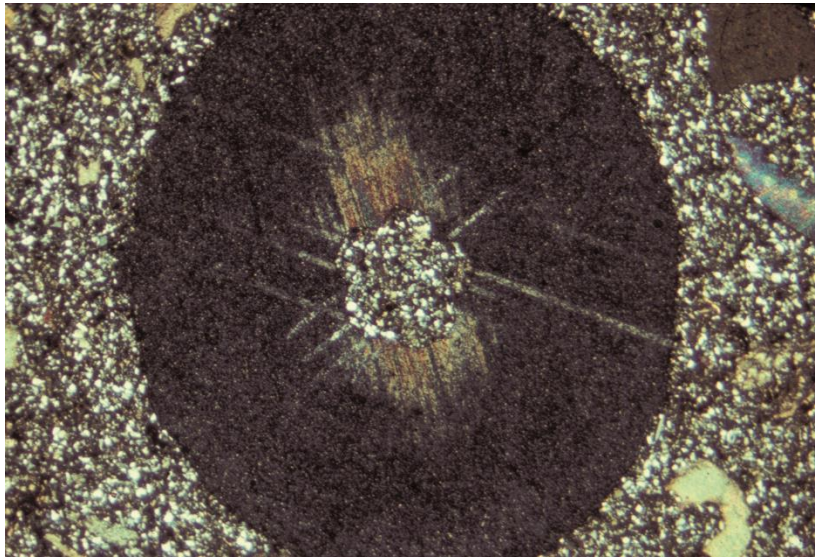

3.1.1 Quantifying Strain: Examples of Shortening

An AAPG Short Course by
Terry Engelder
Professor of Geosciences
The Pennsylvania State University

Compaction of shale around a concretion: 1-D deformation
Devonian Rhinestreet Formation, Dunkirk, New York, USA

Deformation is conveniently separated into three components, of which two are displayed in a one-dimensional analysis. In one dimension there can only be a rigid-body translation (burial) and a stretch (compaction around a concretion is negative stretch). The third component shows up in two and three dimensions where there is an additional deformation known as a rigid-body rotation where the body spins about an axis. Even though this is a 2-D image, the concretion does not ordinarily spin during burial but the shale in the vicinity of the concretion does. For this example we consider the shale at a remote location relative to the concretion.

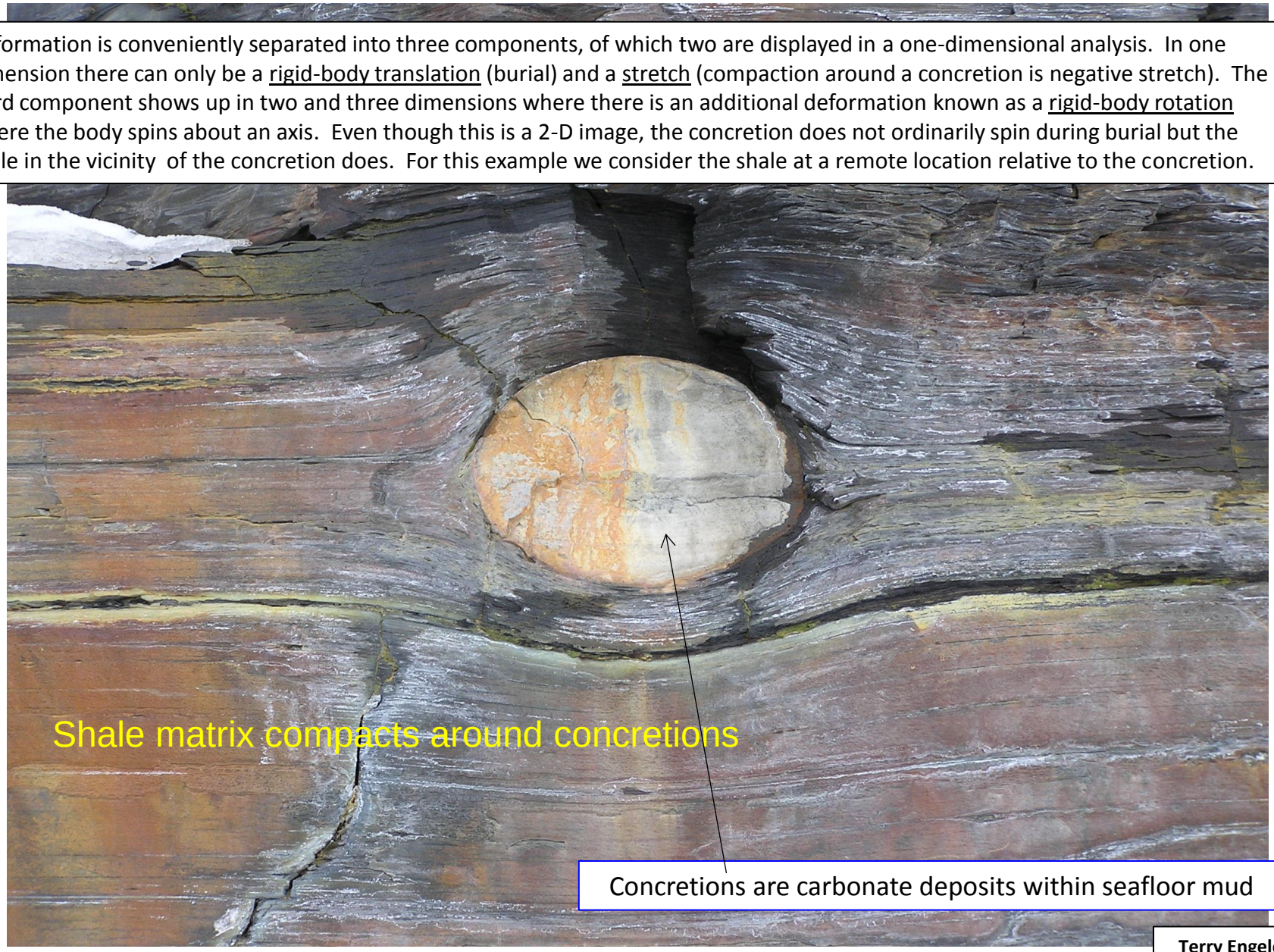

Terry Engelder

1-D strain

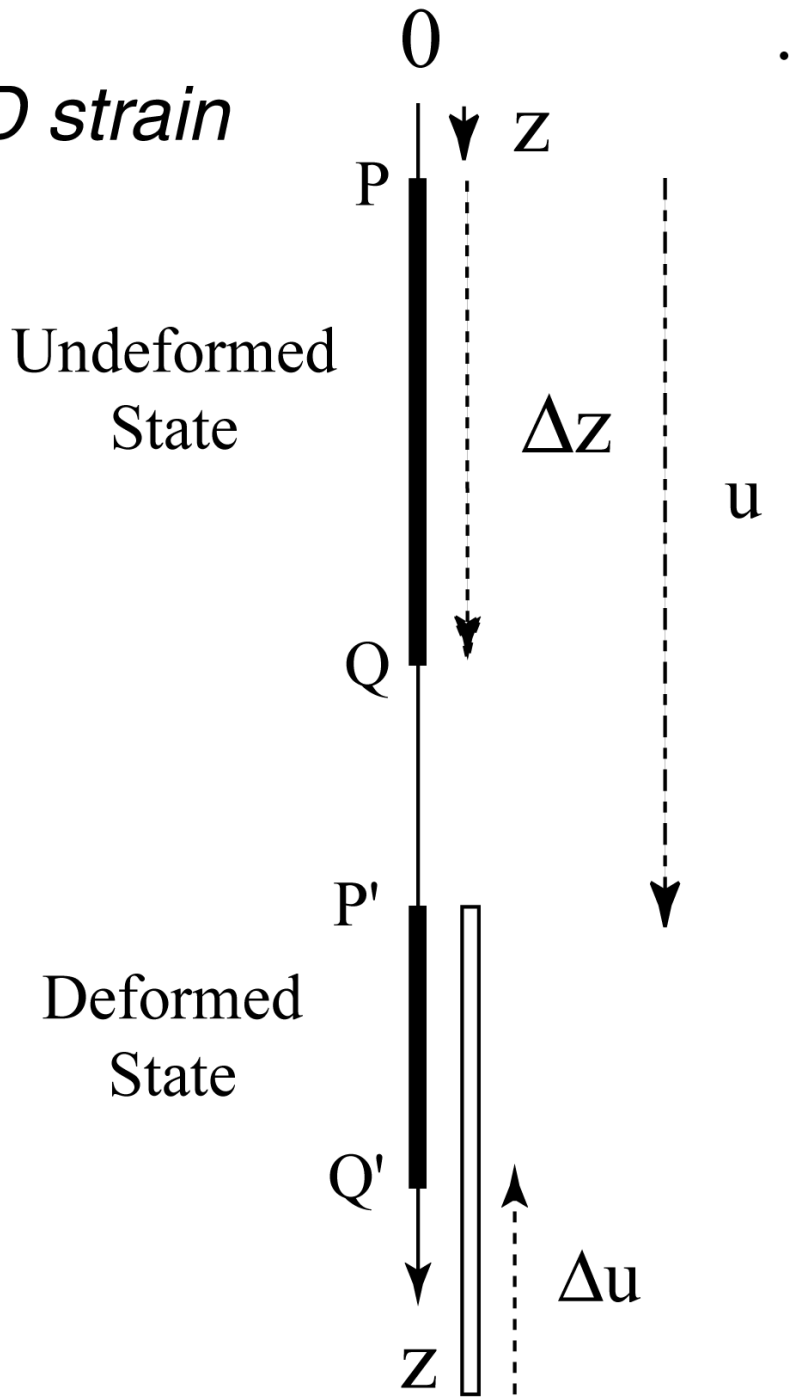

Strain: Change in length over original length --- $(\Delta z - \Delta u)/\Delta z$

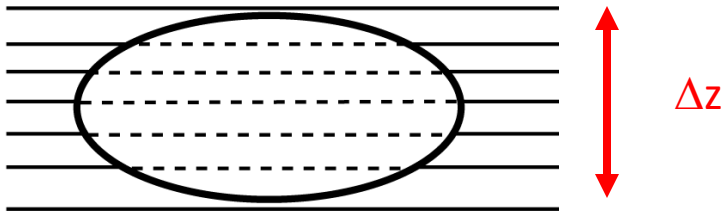

The change in length is commonly referred to as a stretch which can either be positive (longer) or negative (shorter).

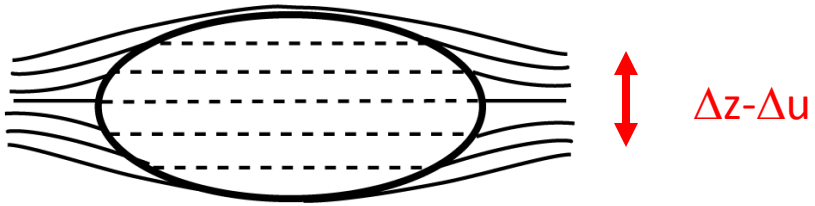

u = displacement in the z direction (unknown)

1-D strain in the horizontal plane

Strain (ε) is a dimensionless quantity defined as a change in length (Δl) per unit length (l).

$$\varepsilon = \Delta l / l$$

Strain is actually defined near a point by the limiting process of differential calculus.

$$\varepsilon = \lim_{l \Rightarrow 0} \left(\Delta l / l \right)$$

Now differential quantities can be introduced by letting $dx = l$ and $du = \Delta l$.

$$\varepsilon = \lim_{\delta x \Rightarrow 0} \frac{\delta u}{\delta x} = \frac{\partial u}{\partial x}$$

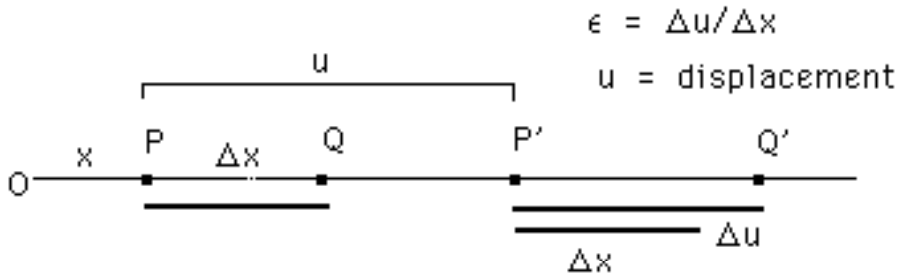

Terry Engelder

Disjunctive Cleavage
Onondaga Limestone, Appalachian Plateau, Geneva, New York, USA

Tectonic Shortening = like compaction it is a negative stretch!

$\varepsilon < 0;\ S < 1$

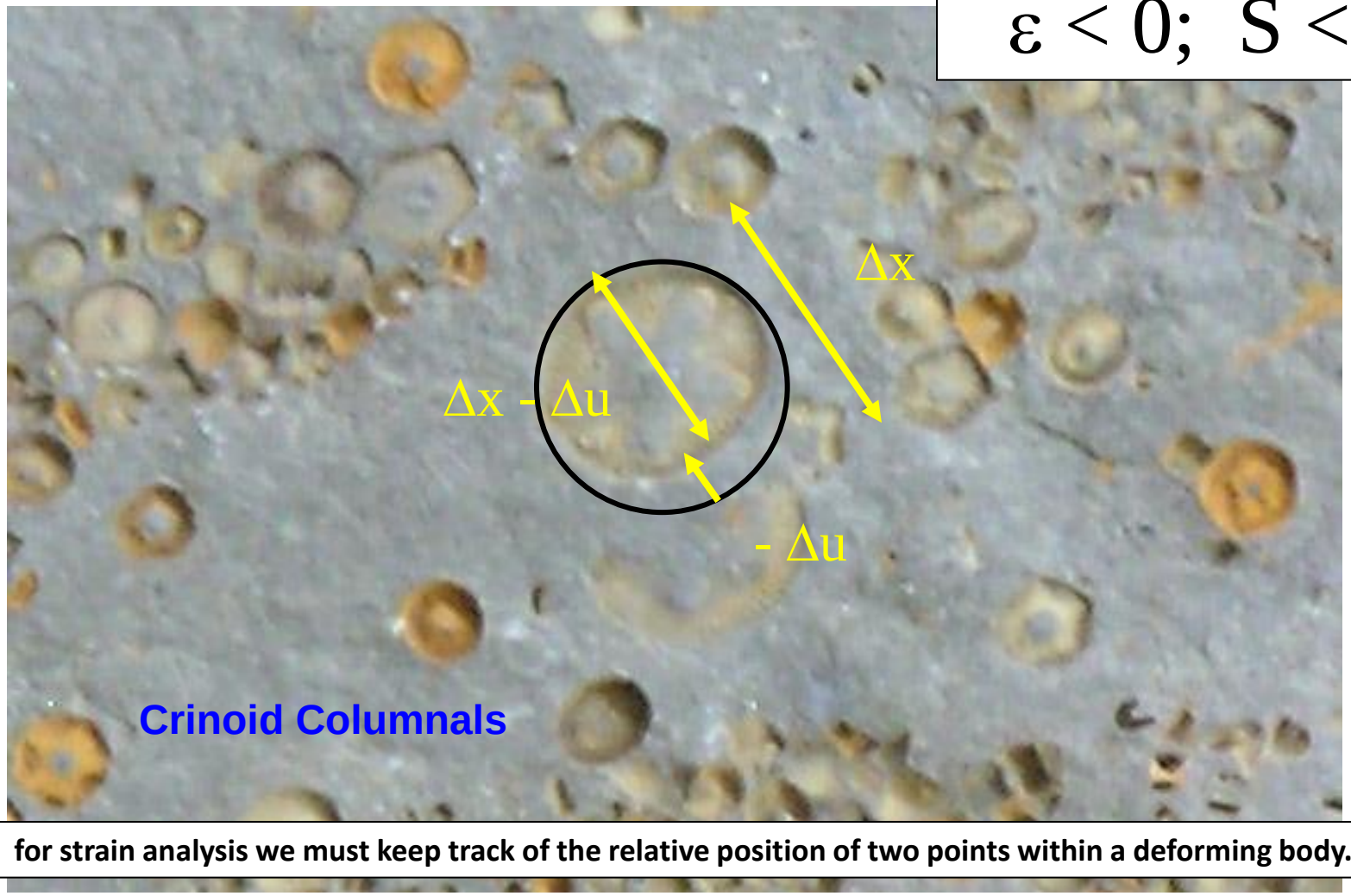

for strain analysis we must keep track of the relative position of two points within a deforming body.

Terry Engelder

2-D and 3-D Deformation Equations

There two techniques for keeping track of what happened to two points within an undeformed body (i.e., the center and edge of a crinoid columnal). First, we can develop a series of equations relating the final resting spot of the point relative to their initial points. Or, we can develop a series of equations describing a vector (red arrow) pointing to the final resting spot from the initial position of a point like center of the crinoid columnal

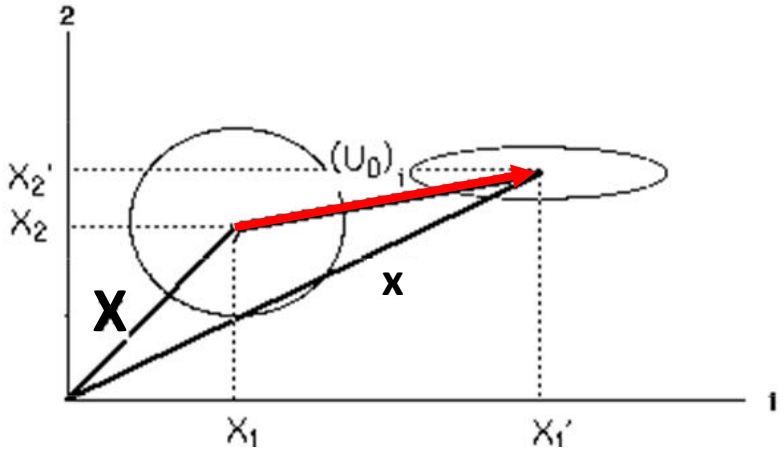

The material point in its undeformed position is specified by a vector **X** with components X_1, X_2, X_3 or X_i. In the new or deformed position the vector **x** has components x_1, x_2, x_3 or x_i

2-Deformation Equations:

$$x_1 = f(X_1, X_2)$$

$$x_2 = f(X_1, X_2)$$

3-Deformation Equations:

$$x_1 = f(X_1, X_2, X_3)$$

$$x_2 = f(X_1, X_2, X_3)$$

$$x_3 = f(X_1, X_2, X_3)$$

A complete deformation includes rigid-translation:

$$x_1 = a_0 + a_1 \cdot X_1 + a_2 \cdot X_2 + a_3 \cdot X_3$$

$$x_2 = b_0 + b_1 \cdot X_1 + b_2 \cdot X_2 + a_3 \cdot X_3$$

$$x_3 = c_0 + c_1 \cdot X_1 + c_2 \cdot X_2 + c_3 \cdot X_3$$

Terry Engelder

2-D and 3-D Deformation Equations

The constants, a_0, b_0, and c_0 specify the rigid-body translation. If there is no rigid-body translation, then the deformation equations for a **homogeneous deformation** may be written in matrix form:

$$\begin{vmatrix} a_1 & a_2 & a_3 \\ b_1 & b_2 & b_3 \\ c_1 & c_2 & c_3 \end{vmatrix}$$

The reason that this is called a homogeneous deformation is that all points x'_i are linearly related to points xi. This is an also example of deformation in plane strain where all motion is parallel to the plane normal to the x_3 axis.

$$x_1 = a_0 + a_1 \cdot X_1 + a_2 \cdot X_2$$

$$x_2 = b_0 + b_1 \cdot X_1 + b_2 \cdot X_2$$

$$x_3 = X_3$$

In contrast a non-homogeneous deformation the points x'_i are related to x_i in a nonlinear manner.

$$x_1 = a_0 + a_1 \cdot X_1 + a_2 \cdot X_2 + a_3 X_1^2$$

$$x_2 = b_0 + b_1 \cdot X_1 + b_2 \cdot X_2 + b_3 X_1^2$$

$$x_3 = X_3$$

Exercise 3.1.1: During the Alpine orogeny a shark's tooth was deformed in the Swiss Alps according to the following deformation equation. Map the deformed shape of the sharks tooth using the following equation!

$$x_1 = 5 + X_1 - X_2$$

$$x_2 = 2X_1 + 2X_2$$

$$x_3 = X_3$$

Terry Engelder

2-D Displacement Equations

The motion of the material point from Xi to xi is also described by a displacement $\mathbf{u}_o$ or $(u_o)_i$. $\mathbf{u}_o$, which is a displacement vector, is nothing more than the final position, **x**, minus the initial position, **X**.

$$(u_0)_1 = x_1 - X_1$$

$$(u_0)_2 = x_2 - X_2$$

$$(u_o)_i = x_i - X_i$$

$$\mathbf{u}_0 = \mathbf{x} - \mathbf{X}$$

The displacement $(u_o)_i$ of the point X_i represents a major part of the motion of all points within a rock body. The motion $(u_o)_i$ is called rigid-body translation because it does not describe the motion of particles or rock relative to each other but rather specifies that all particles follow the same path.

In this brief introduction we have only specified how individual points move during deformation. We have not yet considered the relative motion of the points.

Terry Engelder

2-D and 3-D Deformation

In geology kinematics is the description of the path that rocks took during deformation. It is also the mathematical description of the relative position of two infinitesimal points during the deformation of rocks. Two points can change by translating together, rotating around each other, or changing in distance relative to one another. We shall call such a mathematical description <u>deformation mapping</u>.

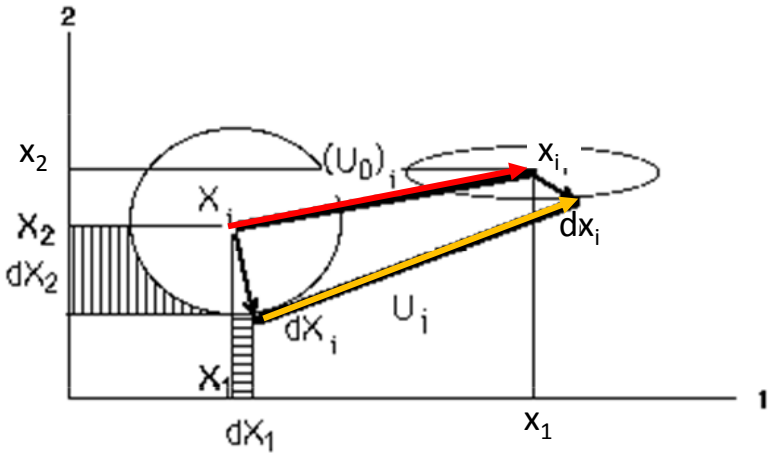

If during rigid-body translation the particles of rock move relative to each other we must devise other equations to account for their relative motion. To the undeformed state we can attach a line segment d**X** whose components are dX_i. The study of deformation is concerned with the change in orientation and length of d**X** as the point at **X** is moved by deformation to the point at **x**. We say that the vector dX_i is both stretched and rotated to become the new vector dx_i. To account for the relative motion of particles within the rock, we consider how the motion u_i of any vector d**X** differs from the motion $(u_o)_i$ of the vector **X**

If $x_i = f(X_j)$ then $x_i + \Delta x_i = f(X_j + \Delta X_j)$ And by a Taylor's expansion $\Delta x_i = (\partial x_i / \partial X_j)\, \Delta X_j$

Terry Engelder

Deformation and Displacement Gradient

$\partial x_i/\partial X_j$ are coefficients called the deformation gradient and are a function of the location within the rock (X_i). The coefficients for the deformation of the shark's tooth are:

$$\left|\frac{\partial x_1}{\partial x_j}\right| = \begin{vmatrix} 1 & -1 & 0 \\ 2 & 2 & 0 \\ 0 & 0 & 1 \end{vmatrix}$$

The displacement gradient, E_{ij}, is a function of position within the rock: $E_{ij} = \partial u_i/\partial x_j$

These scalar quantities, E_{ij}, are the components of the displacement equations which take the following form:

$$u_1 = \frac{\partial u_1}{\partial X_1} X_1 + \frac{\partial u_1}{\partial X_2} X_2 + \frac{\partial u_1}{\partial X_3} X_3$$

$$u_2 = \frac{\partial u_2}{\partial X_1} X_1 + \frac{\partial u_2}{\partial X_2} X_2 + \frac{\partial u_2}{\partial X_3} X_3$$

$$u_3 = \frac{\partial u_3}{\partial X_1} X_1 + \frac{\partial u_3}{\partial X_2} X_2 + \frac{\partial u_3}{\partial X_3} X_3$$

or

$$u_1 = (u_0)_1 + E_{11}dX_1 + E_{12}dX_2 + E_{13}dX_3$$

$$u_2 = (u_0)_2 + E_{21}dX_1 + E_{22}dX_2 + E_{23}dX_3$$

$$u_3 = (u_0)_3 + E_{31}dX_1 + E_{32}dX_2 + E_{33}dX_3$$

Deformation is separated into three components: rigid-body translation, stretch and rigid-body rotation.

Stretch = $\varepsilon_{ij} = {}^1/_2 (E_{ij} + E_{ij})$

Rigid-body rotation = $\omega_{ij} = {}^1/_2 (E_{ij} - E_{ij})$.

Geological Deformation

Exercise #2 The first deformation to occur in the history of a sedimentary rock is overburden compaction. This is represented by flattening in the vertical direction with no deformation in the horizontal directions. Compaction around a concretion was used to illustrate this deformation. The following equations represent overburden compaction. Where does the underformed point X_i = [1,1,1] end up after compaction (we say that the initial point is mapped to the final point using the displacement equations)? What is the vector connecting the undeformed point X_i = [1,1,1] to its deformed counterpart? Hint: See figure for deformation!

Displacement equations:

$$u_1 = 0X_1 + 0X_2 + 0X_3$$
$$u_2 = 0X_1 + 0X_2 + 0X_3$$
$$u_3 = 0X_1 + 0X_2 - 0.5X_3$$

Deformation equations:

$$x_1 = 1X_1 + 0X_2 + 0X_3$$
$$x_2 = 0X_1 + 1X_2 + 0X_3$$
$$x_3 = 0X_1 + 0X_2 + 0.5X_3$$

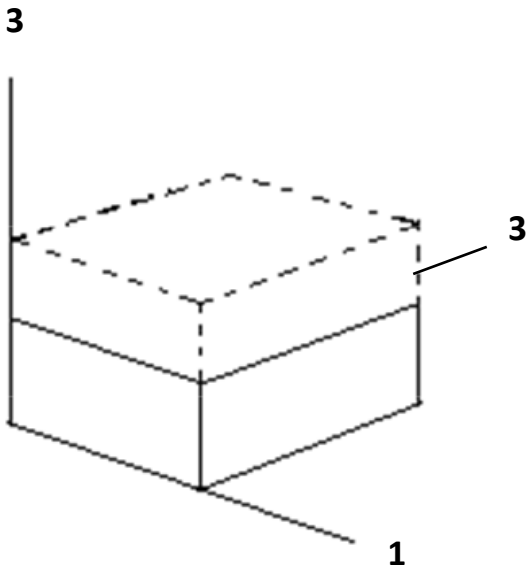

Terry Engelder

2-D and 3-D Deformation

Exercise #3: If the compacted shale from Exercise #2 were turned on its side this deformation could represent a tectonic compaction. The Martinsburg shales near Harrisburg, Pennsylvania, have been isoclinally folded. Beds which were once flat-lying are now standing on end with a dip of 90°. Assuming that the shales were deformed with no internal strain we can use the following equations represent the rigid rotation of a block of shale by 90°. Where does the underformed point X_i = [1,1,1] end up after rigid-body rotation (we say that the initial point is mapped to the final point using the displacement equations)? What is the vector connecting the shale at point X_i = [1,1,1] to its rotated counterpart? Hint: See figure for this deformation!

Displacement equations (A vector from the old point to its new location):

$$
\begin{aligned}
u_1 &= 0X_1 + 0X_2 + 0X_3 \\
u_2 &= 0X_1 - 1X_2 - 1X_3 \\
u_3 &= 0X_1 + 1X_2 - 1X_3
\end{aligned}
$$

Deformation equations (A map of the new point given the coordinates of its old position):

$$
\begin{aligned}
x_1 &= 1X_1 + 0X_2 + 0X_3 \\
x_2 &= 0X_1 + 0X_2 - 1X_3 \\
x_3 &= 0X_1 + 1X_2 + 0X_3
\end{aligned}
$$

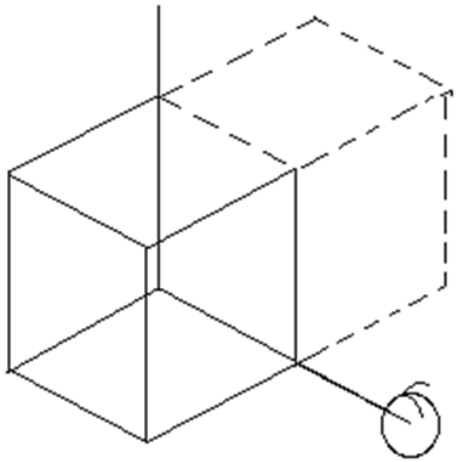

Terry Engelder

2-D and 3-D Deformation

Exercise #4 As a final review of deformation and displacement equations, we shall take a look at the behavior of a fault zone subject to simple shear. In higher grade terrains these fault zones are simply called shear zones. The deformation and displacement equations are given below. Where does the point X_i = [1,1,1] end up after simple shear in a fault zone (we say that the initial point is mapped to the final point using the displacement equations)? What is the vector connecting the fault at point X_i = [1,1,1] to its sheared counterpart? Hint: See figure for this deformation!

Displacement equations (A vector from the old point to its new location):

$$u_1 = 0X_1 + 0X_2 + 0X_3$$
$$u_2 = 0X_1 + 0X_2 + 0.5X_3$$
$$u_3 = 0X_1 + 0X_2 + 0X_3$$

Deformation equations (A map of the new point given the coordinates of its old position):

$$x_1 = 1X_1 + 0X_2 + 0X_3$$
$$x_2 = 0X_1 + 1X_2 + 0.5X_3$$
$$x_3 = 0X_1 + 0X_2 + 1X_3$$

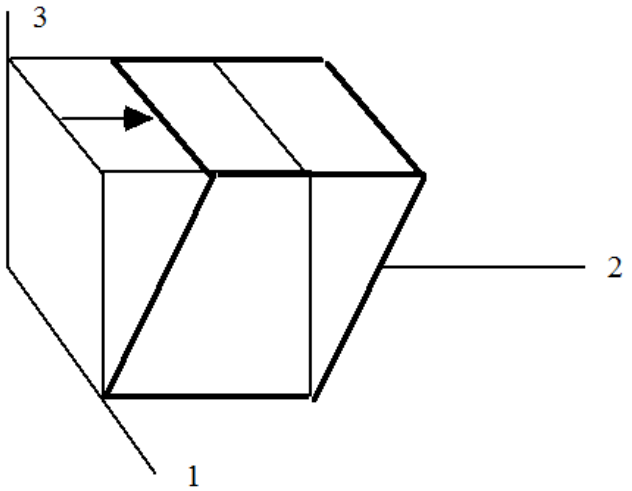

Terry Engelder

A formal definition of shear strain (γ) is the change in angle (ψ) between two initially perpendicular lines

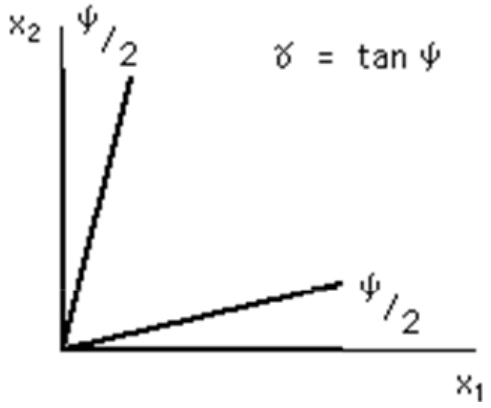

A second measure of shear strain is the tensor shear strain which is half the tangent of the change in angle between initially perpendicular lines

$$\text{Tensor shear strain} = \gamma/2.$$

Shear strain (γ) is also called engineering shear strain

The following are useful definitions

$\varepsilon = \Delta l/l_0$	(elongation)
$S = l_1/l_0 = (1+\varepsilon)$	(stretch)
$\lambda = (l/l_0)^2 = (1+\varepsilon)^2$	(quadratic elongation)
$\varepsilon = dl/l_0$	(infinitesimal strain)
$\varepsilon = \Delta l/l_0$	(small increment of strain)
$\varepsilon = \int_{l_0}^{l_1} dl/l_0 = \ln(l_1/l_0) = \ln(1+\varepsilon) = {}^1/_2\ln\lambda$	(natural strain)

Irrotational vs. Rotational Strain

The rotational strain tensor, e_{ij}, applies to infinitesimal strains and is a general (or asymmetric) second rank tensor and can be expressed as the sum to a symmetric and an antisymmetric tensor:

$$e_{ij} = \varepsilon_{ij} + \omega_{ij} \qquad \text{where} \qquad \varepsilon_{ij} = \frac{1}{2}(e_{ij} + e_{ji}) \qquad \text{and} \qquad \omega_{ij} = \frac{1}{2}(e_{ij} - e_{ji})$$

These simple definitions help us understand the distinctions between simple shear and pure shear. Overburden compaction is a case of pure shear with the deformation gradient matrix:

$$\frac{\partial u_i}{\partial x_j} = \begin{vmatrix} 0 & 0 & 0 \\ 0 & 0 & 0 \\ 0 & 0 & -0.005 \end{vmatrix}$$

The rotational strain tensor, e_{ij}, is

$$e_{ij} = \begin{vmatrix} 0 & 0 & 0 \\ 0 & 0 & 0 \\ 0 & 0 & -0.005 \end{vmatrix}$$

The irrotational strain tensor, ε_{ij}, is

$$\varepsilon_{ij} = \begin{vmatrix} 0 & 0 & 0 \\ 0 & 0 & 0 \\ 0 & 0 & -0.005 \end{vmatrix}$$

The rotational component of strain is

$$\omega_{ij} = \begin{vmatrix} 0 & 0 & 0 \\ 0 & 0 & 0 \\ 0 & 0 & 0 \end{vmatrix}$$

For pure shear there is a remarkable similarity between the rotational strain tensor and the irrotational strain tensor. This similarity disappears for the case of simple shear.

Terry Engelder

Irrotational vs. Rotational Strain

The deformation gradient matrix and the rotational strain tensor for simple shear in a fault zone is

$$\frac{\partial u_i}{\partial x_j} = e_{ij} = \begin{vmatrix} 0 & 0 & 0 \\ 0 & 0 & 0.05 \\ 0 & 0 & 0 \end{vmatrix}$$

The irrotational strain tensor, ε_{ij}, is

$$\varepsilon_{ij} = \begin{vmatrix} 0 & 0 & 0 \\ 0 & 0 & 0.025 \\ 0 & 0.025 & 0 \end{vmatrix}$$

The rotational component of strain is

$$\omega_{ij} = \begin{vmatrix} 0 & 0 & 0 \\ 0 & 0 & 0.025 \\ 0 & -0.025 & 0 \end{vmatrix}$$

The distinction between pure shear and simple shear is further clarified by considering the principal strain axes. If the directions of the principal axes of strain do not change as a result of displacement, then that deformation is termed irrotational strain. In the case of simple shear the principal axes of strain always differ depending on the amount of shear. The difference defines the rotational component of strain which is known as rotational strain. It is important to note that although simple shear is a rotational deformation, there has been no actual rotation in space within a fault zone. The development of rotational strain does not necessarily imply that the body has to spin physically around some axis. Because of this lack of real rotation of within a fault zone, some like to refer to the rotation as an internal rotation. This type of rotation is in contrast to our example of external rotation where bedded sediments being turned on end as given previously by the displacement equations.

Terry Engelder


15% Layer-Parallel Shortening


15% Layer-Parallel Shortening

Layer parallel shortening
Appalachian Plateau, New York, USA

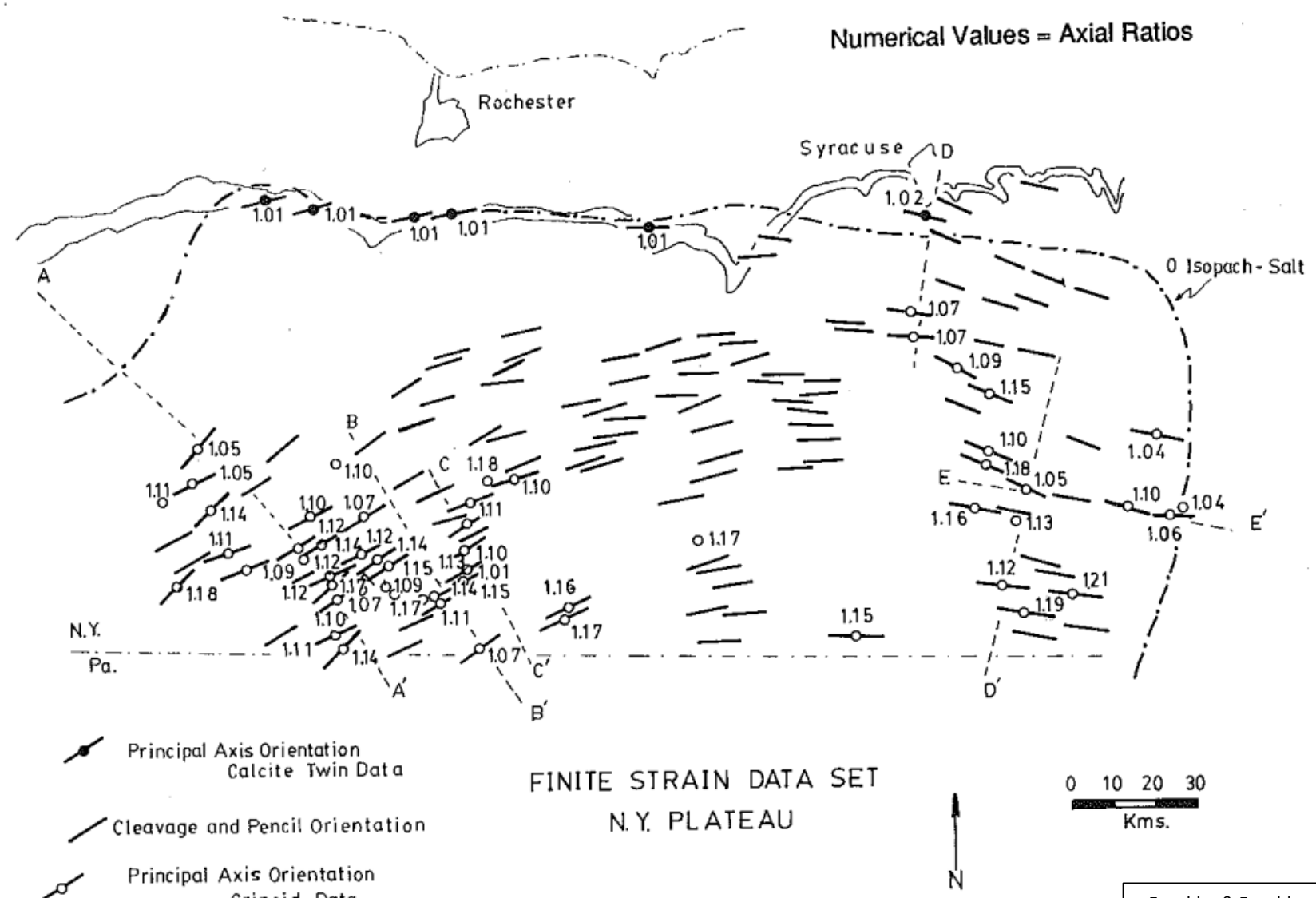

Engelder & Engelder, 1977
Engelder & Geiser, 1979
Geiser, 1988

Disjunctive Cleavage

Onondaga Limestone, Appalachian Plateau, Geneva, New York, USA

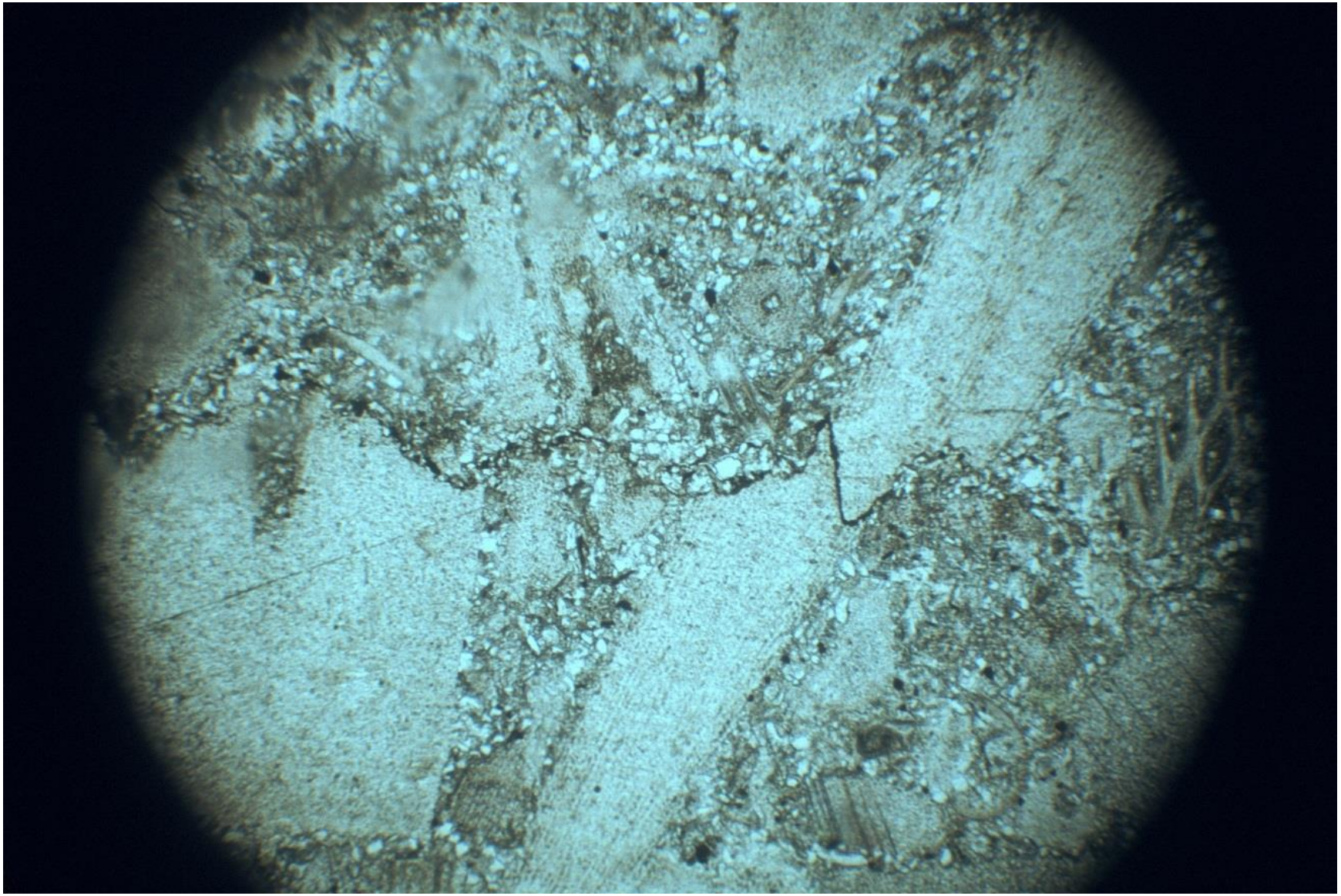

Terry Engelder

Disjunctive Cleavage on edge of Crinoid Columnal
Canadaway Formation, Appalachian Plateau, Wellsville, New York, USA

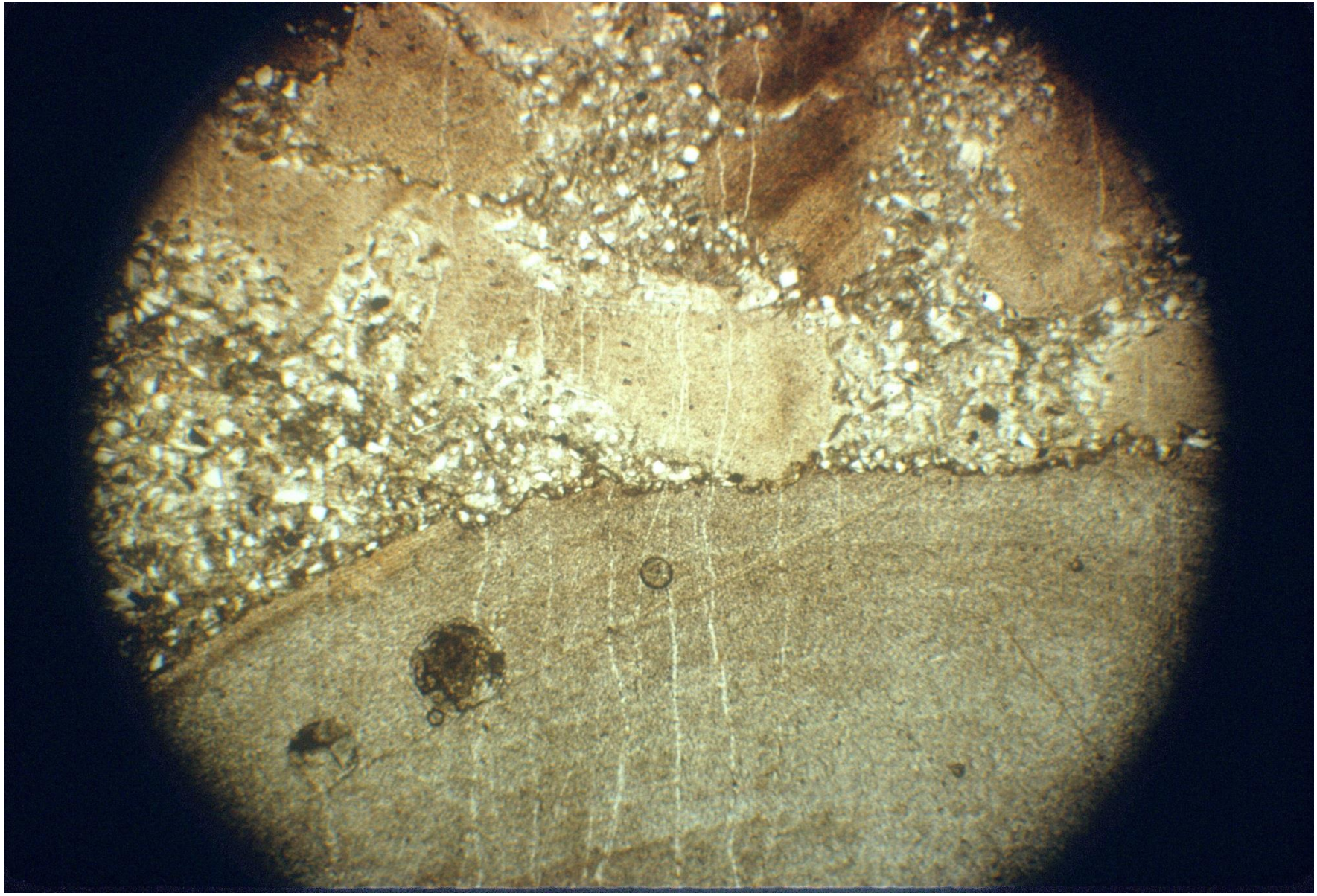

Terry Engelder

Layer parallel shortening
Appalachian Plateau, New York, USA

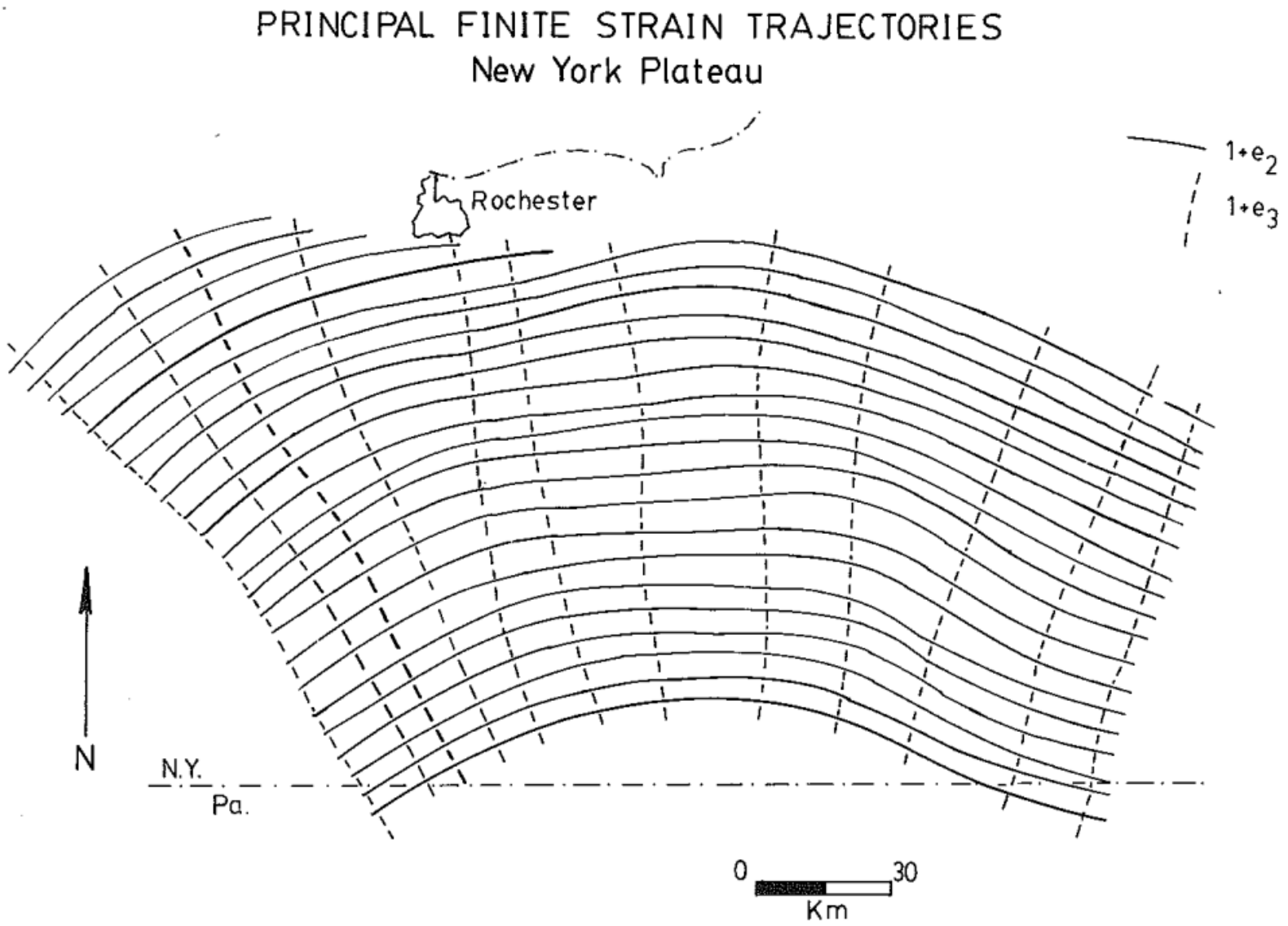

Geiser, 1988

Iso-strain map prepared from strain data
Appalachian Plateau, New York, USA

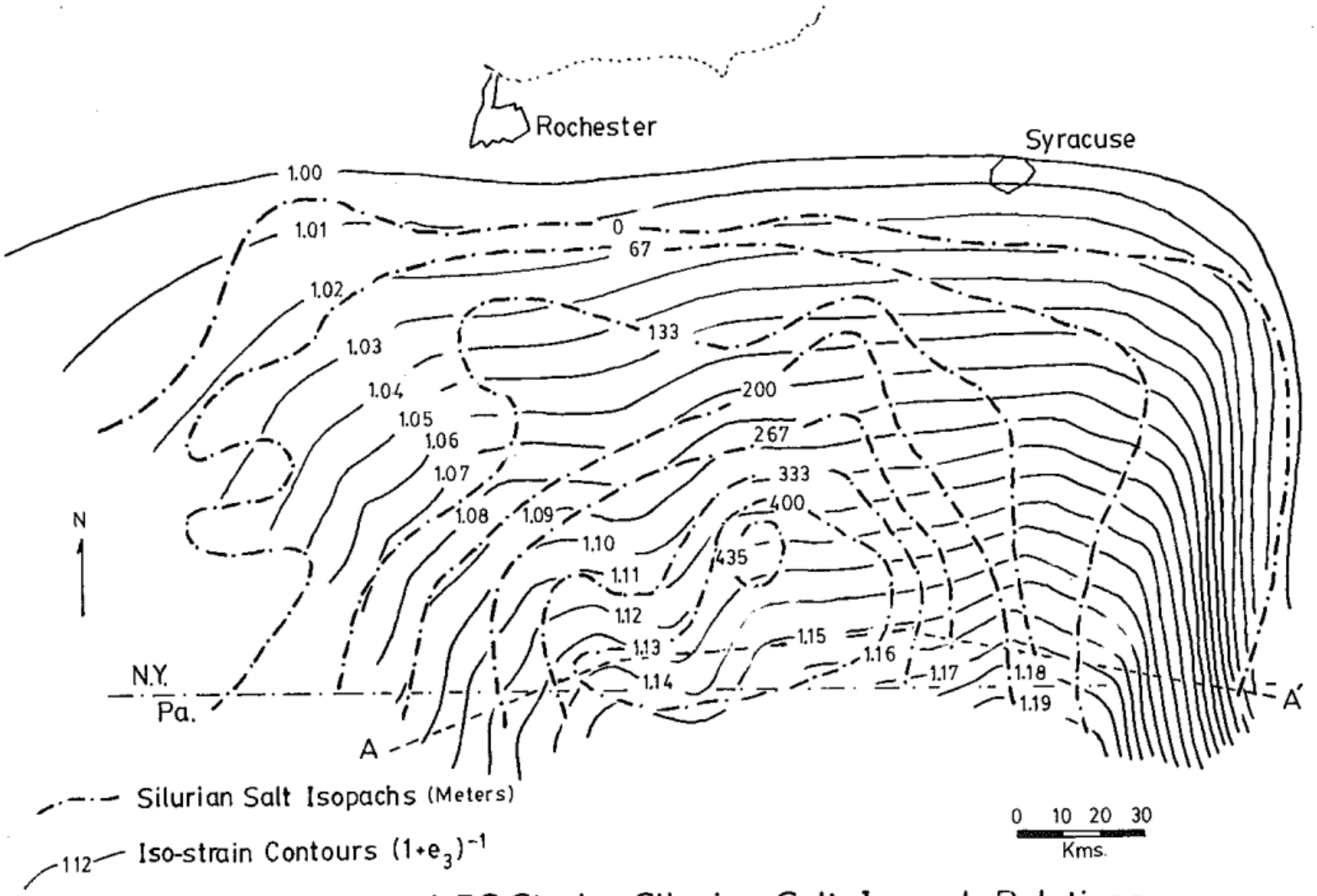

LPS Strain - Silurian Salt Isopach Relations
NY Plateau

Geiser, 1988

Deformed Grid
Appalachian Plateau, New York, USA

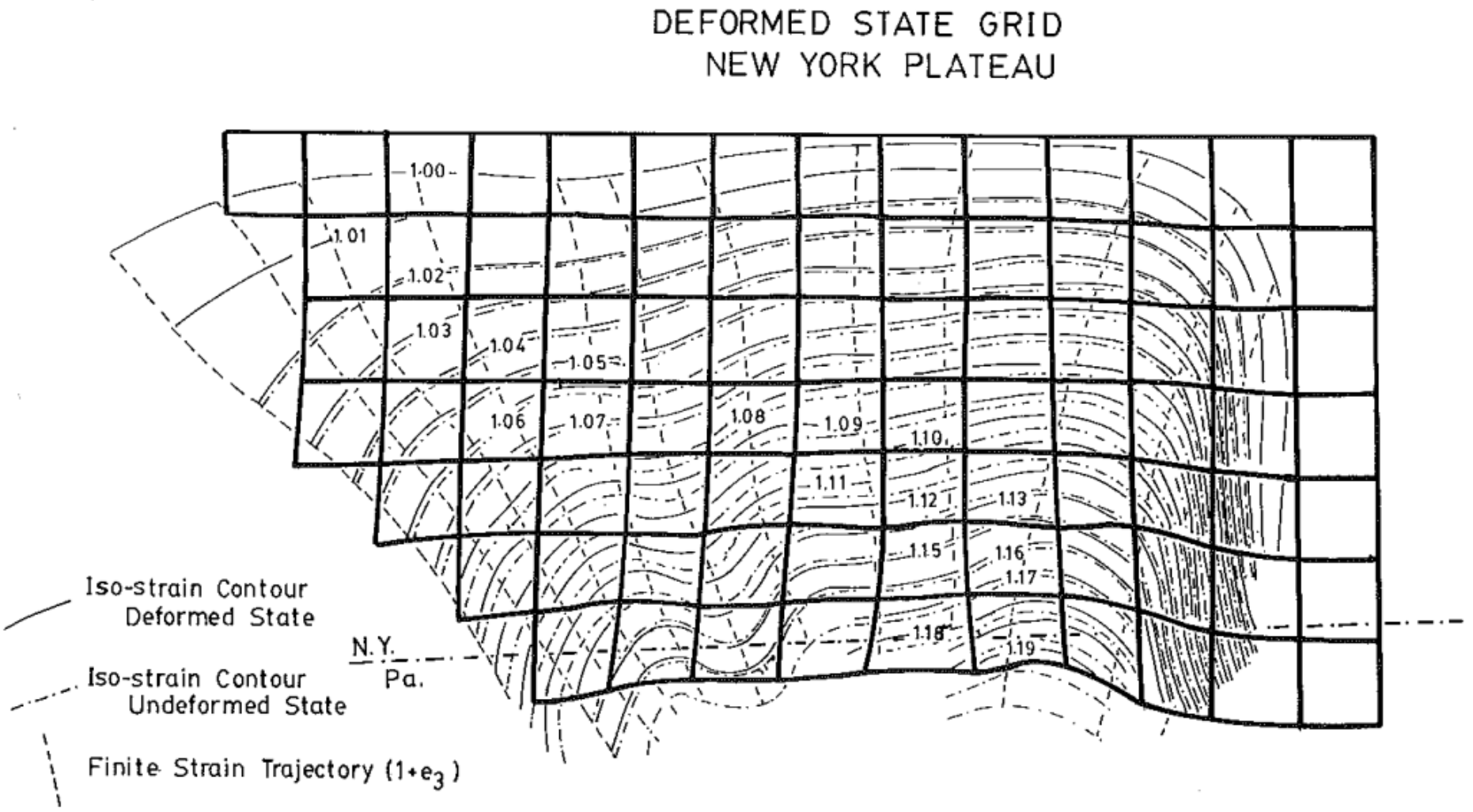

Geiser, 1988

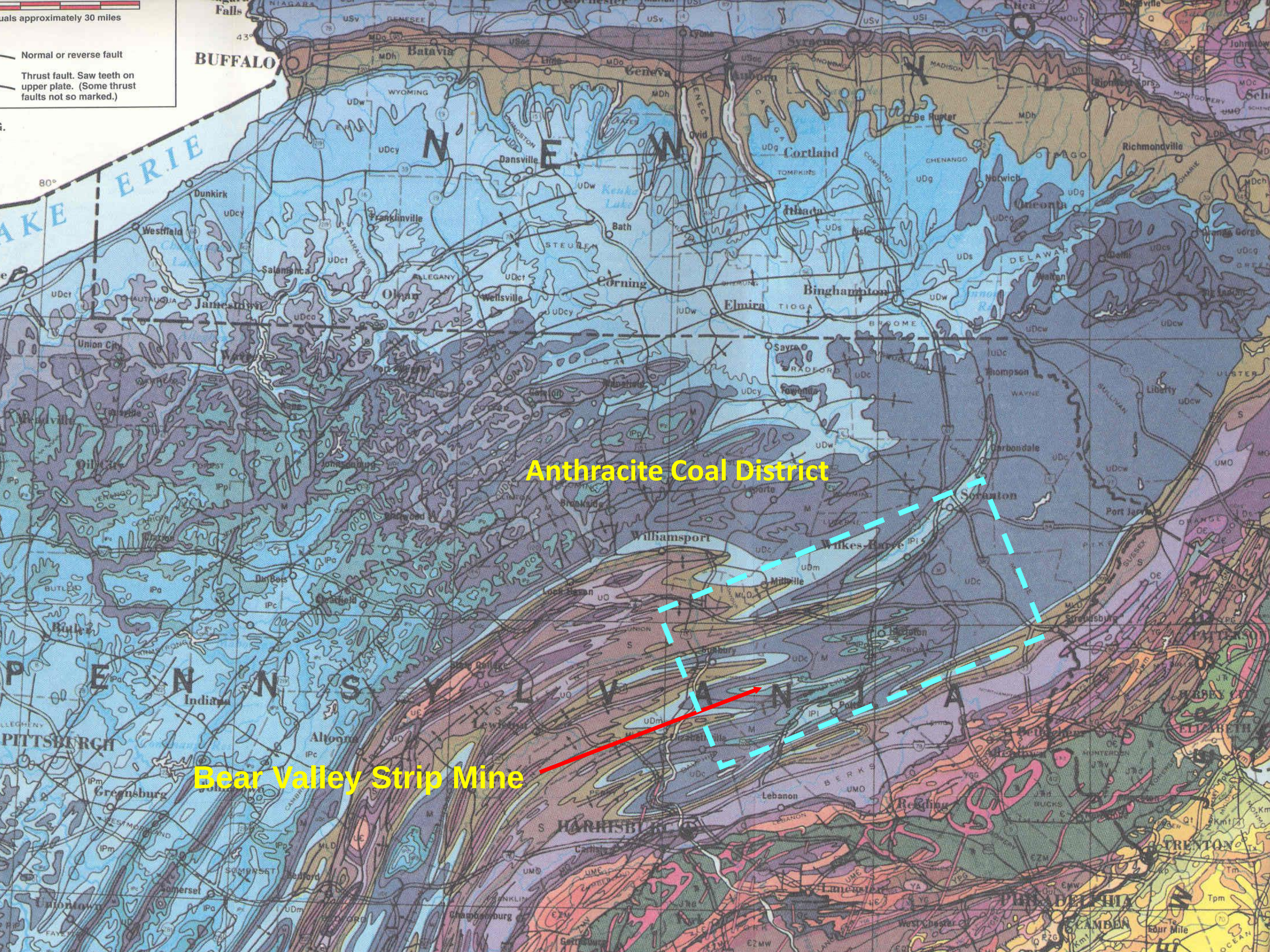

uals approximately 30 miles
Normal or reverse fault
Thrust fault. Saw teeth on upper plate. (Some thrust faults not so marked.)
BUFFALO
LAKE ERIE
NEW
PENNSYLVANIA
Anthracite Coal District
Bear Valley Strip Mine
Batavia
Geneva
Auburn
Cortland
Ithaca
Binghamton
Elmira
Corning
Olean
Jamestown
Dunkirk
Westfield
Salamanca
Wellsville
Dansville
Bath
Norwich
Oneonta
Richmondville
Williamsport
Wilkes-Barre
Scranton
Carbondale
Towanda
Sayre
Thompson
Liberty
Port Jervis
Stroudsburg
Milleville
Sunbury
Lewistown
Altoona
Indiana
Greensburg
PITTSBURGH
Butler
Oil City
HARRISBURG
Lebanon
Reading
TRENTON
PHILADELPHIA
CAMDEN
Lancaster
Chambersburg
Somerset
Uniontown
Lock Haven

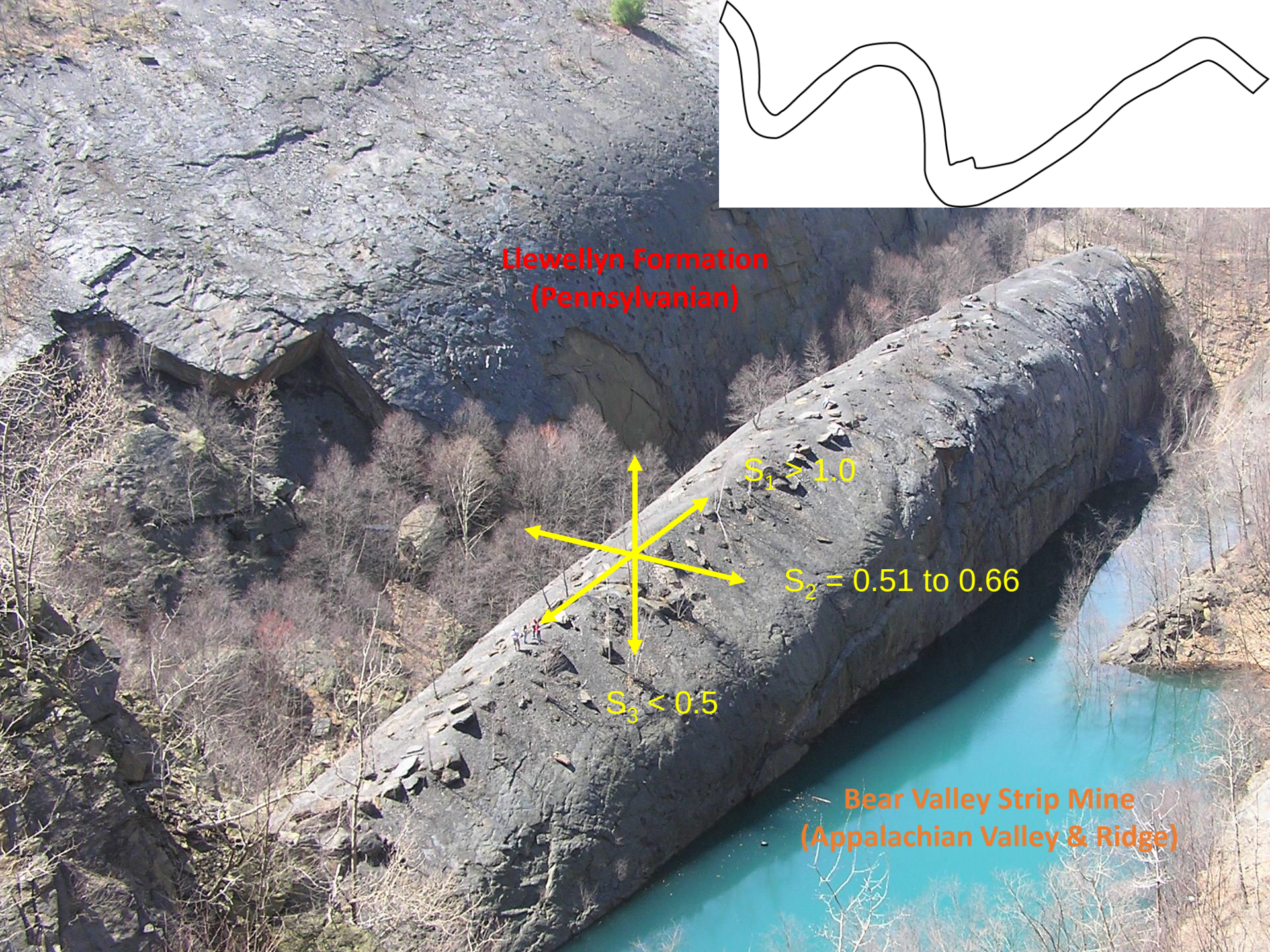
Llewellyn Formation
(Pennsylvanian)
$S_1 > 1.0$
$S_2 = 0.51$ to 0.66
$S_3 < 0.5$
Bear Valley Strip Mine
(Appalachian Valley & Ridge)

Tectonic Compaction

- Tectonic Compaction is a process that brings about a **layer-parallel shortening**, with a further **decrease in pore volume.** During tectonic compaction there is also **a net change in water content.** The degree of compaction depends on structural position within the orogenic belt.

Concretions on a bedding plane

lycopsid branch captured by concretion (S_2 = 0.78)

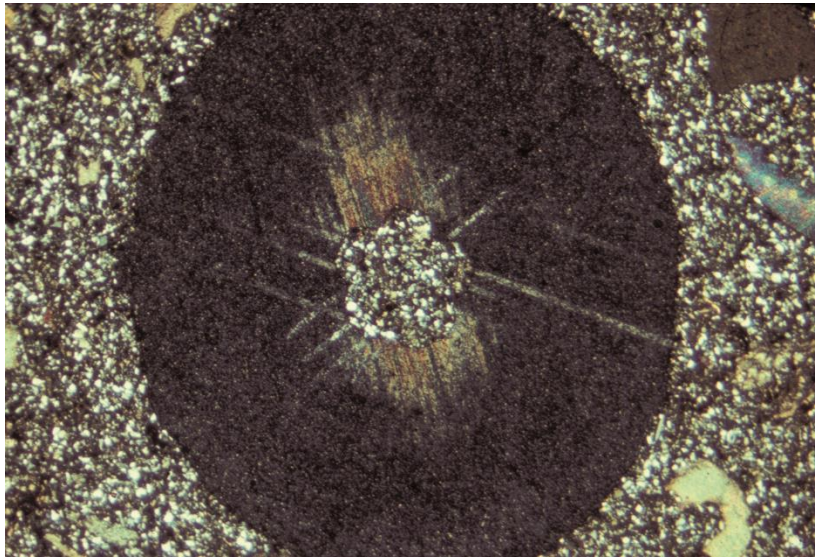

3.1.2 – Strain Markers: Examples of Extension

An AAPG Short Course by
Terry Engelder
Professor of Geosciences
The Pennsylvania State University

Basin and Range, USA

Deformation and then strain were introduced in the context of mechanical and then chemical compaction during burial. This leads to a stretch which is less than one. Furthermore, in a foreland like the Appalachian Plateau a tectonic compaction takes place which means there is a stretch of less than one in the direction of layer-parallel shortening. In other tectonic settings there is an extension which means that stretch is greater than one. In considering more strain markers outside those found on the Appalachian Plateau, a positive stretch is common. We start with an example of regional stretch by normal faulting, the Basin and Range, USA, where the unstrained upper crust was about half it present length along a line from Carson City Nevada to Salt Lake City.

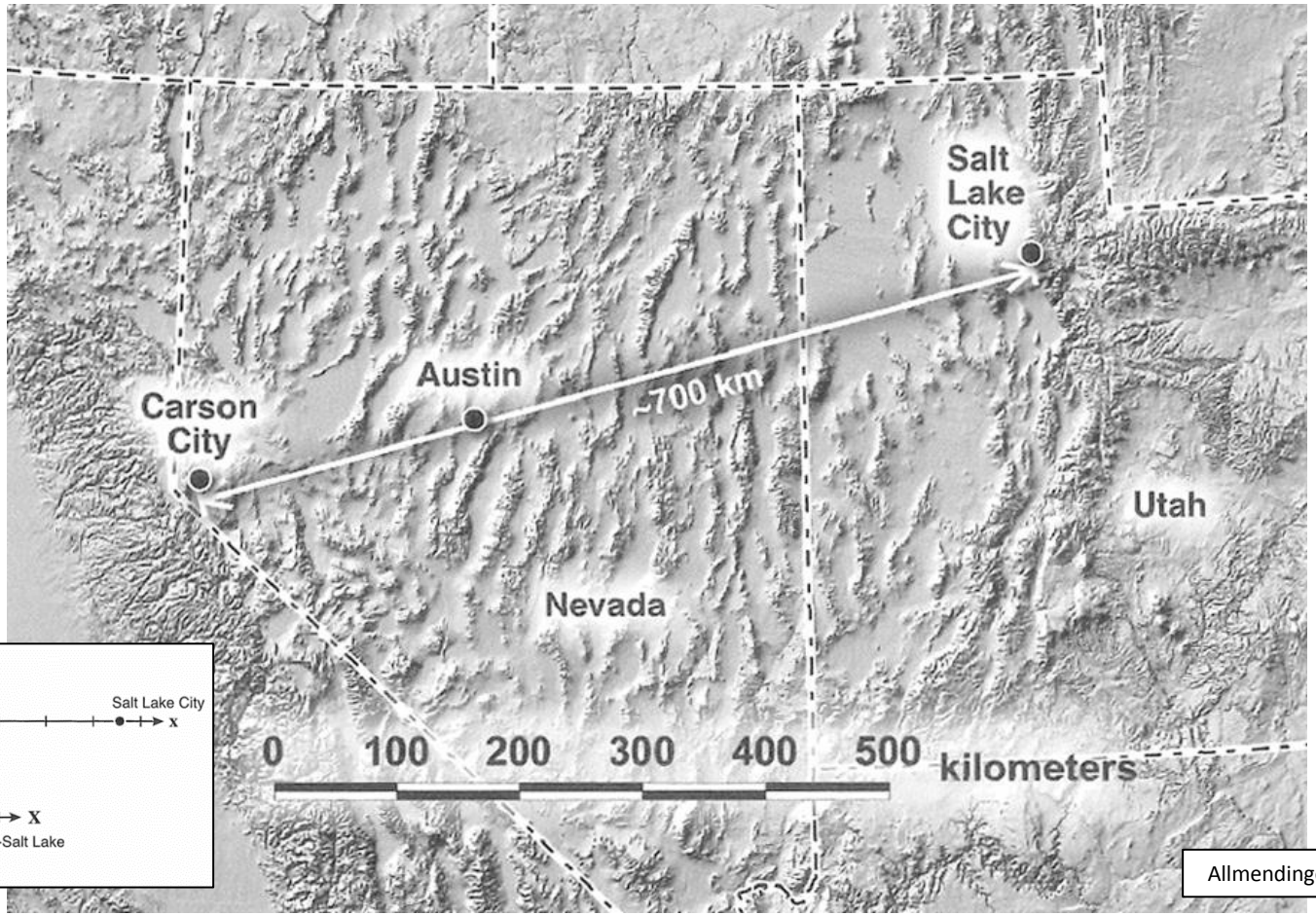

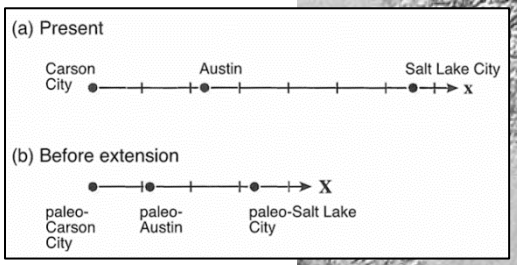

Allmendinger et al., 2012

Progressive deformation
Extension Veins

In studying deformation and strain for extension of the Basin and Range and layer parallel shortening of the Appalachian Plateau detachment sheet, all we could do was compare the final shape (line length) with its initial shape (line). There was no information about intermediate deformation yet we know from the propagation of multiple joint sets that the orientation of principal stress change during tectonic deformation and in this case it is unlikely that the orientation of incremental strain was the same for each step. This is in contrast with invariant stress orientation during compaction accompanying burial where strain is described as **coaxial** or pure shear. When stress orientation changes over time, the geometry of deformation changes in a progressive way and we say that the strain is **non coaxial**. We call this progressive deformation which is most easily seen in the way that fibers grow in extension veins and stress shadows.

The fiber growth in extension has have four geometries. In syntaxial veins the fiber material is very close or identical to the composition of grains in walls. Often the fibers grow in crystallographic continuity with the wall rock grains and growth of the veins takes place at the medial line. The common sedimentary rocks find that syntaxial fibers in carbonates are calcite and in sandstone they are quartz. Antitaxial fibers commonly entrain wall rock along a central band and have no crystallographic relationship with the wall. Growth of these fibers is toward the wall and commonly the wall is fractured a number of times with the incorporation of a number of fragment trains in a process called **crack seal** (Ramsay, 1980). Sometime a vein may display a combination of both antitaxial and syntaxial growth (a composite vein). In some instances the fibers are straight but at an angle to the wall which means the opening direction did not change with time.

Black and white crystals represent different orientations of the crystalline lattice. Arrows indicate the direction of fiber growth. Drawings from Ramsay and Huber, 1983

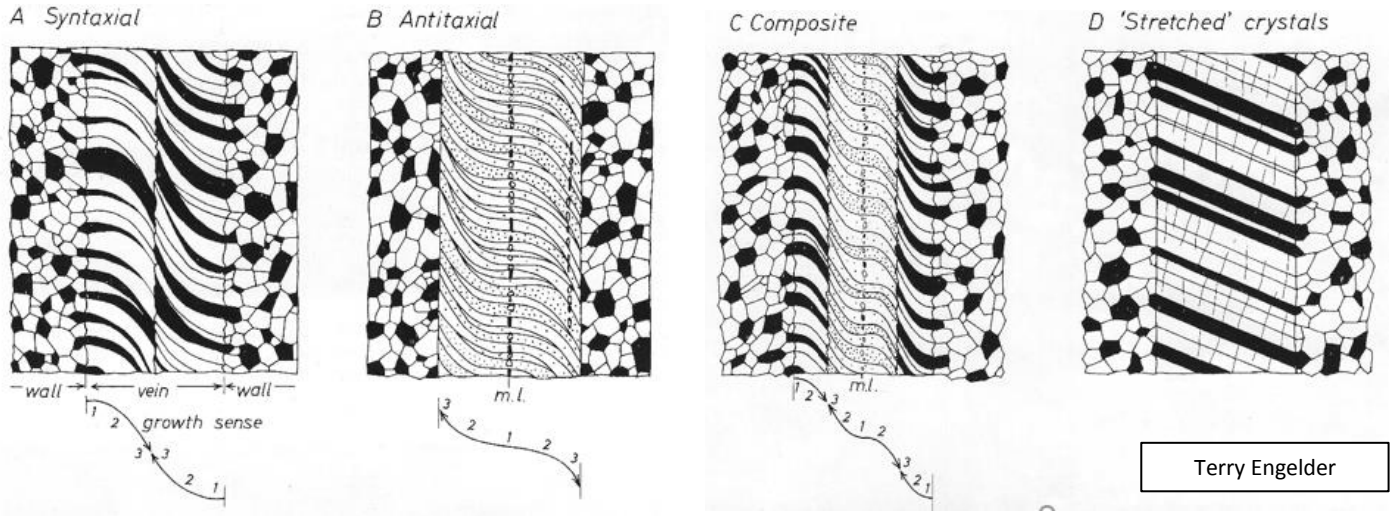

Terry Engelder

Progressive deformation
Pressure Shadows

Some sedimentary rocks contain inclusions that resist deformation relative to their matrix. We have already seen that carbonate concretions fail to compact as overburden is added, layer by layer. Pyrite framboids are also strong relative to a clay of a shale matrix. This relative strength is preserved through lithification as indicated by matrix detaching from concretions during tectonic compaction. Some inclusions are more susceptible to deformation along with the rock matrix as is the case with crinoid columnals during layer-parallel shortening.

Rigid inclusions respond much like the walls of a vein during extension in that there can be either syntaxial or antitaxial growth in pressure shadows. In the case of rigid inclusions the pyrite pressure shadows grow in crystallographic continuity with the wall rock which means the fiber growth takes place at the fiber-framboid contact (i.e., syntaxial growth). The fiber growth for crinoid type pressure shadows takes place at the contact between the pressure shadow and the wall rock. In the drawing on this page, the crinoid is a single crystal that has been mechanically twinned during tectonic deformation. Pressure shadows indicate either coaxial strain (straight fibers) or non-coaxial strain (curving fibers).

Arrows give an indication of the direction of fiber growth. Drawing taken from Ramsay and Huber, 1983.

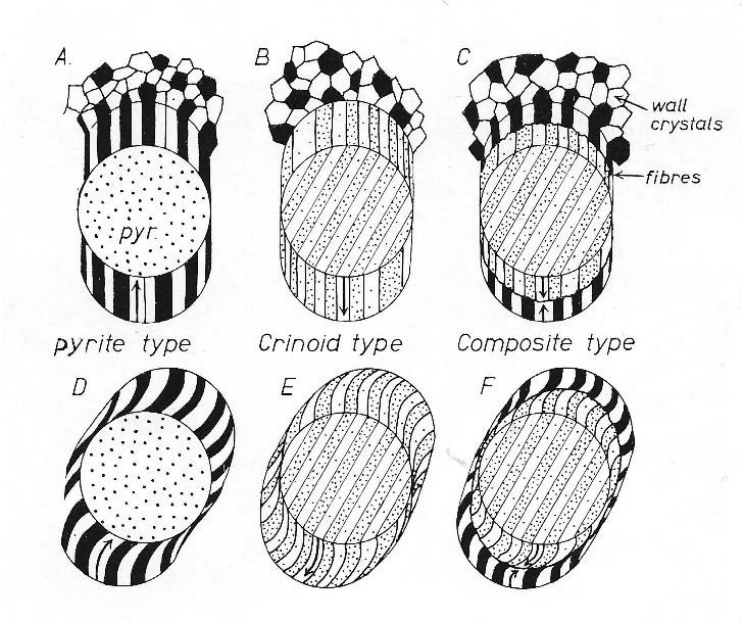

Terry Engelder

name
place

When the growth of the fiber pressure shadow is at the rigid inclusion, such as against pyrite, this is said to be an example of **displacement controlled fibers**. For example, in the figure to the right, fibers grew on the left wall at time a. But because extension rotated clockwise and shifted away from the left wall as fiber growth continued growth, the initial growth was displaced away from the wall. Eventually growth continued on the left wall but in a different direction.

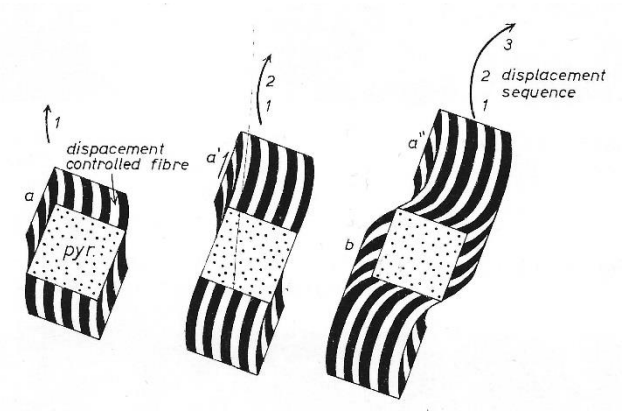

Two fiber growth models are possible during coaxial strain (straight fibers). A rigid fiber growth model presumes that the fibers are not deformable so each increment is identical (model B). If the fibers are deformable then the outline of the fibers (model C) takes the shape of the strain ellipse (outline A).

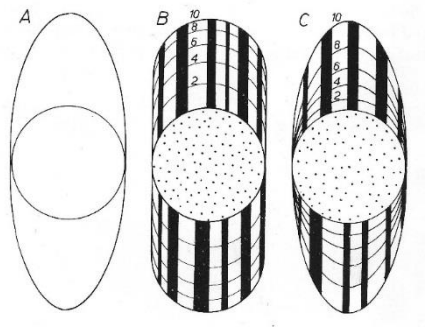

Two fiber growth models are possible during non coaxial strain (curved fibers). A rigid fiber growth model presumes that the fibers are not deformable so each increment is identical (model B). If the fibers are deformable then the outline of the fibers (model C) takes the shape of the strain ellipse (outline A).

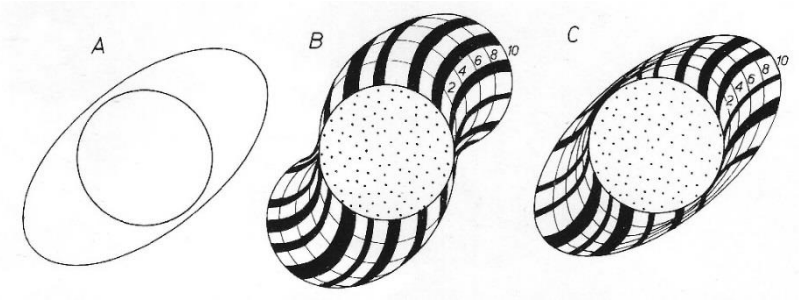

Drawings after Huber and Ramsay (1983)

Terry Engelder

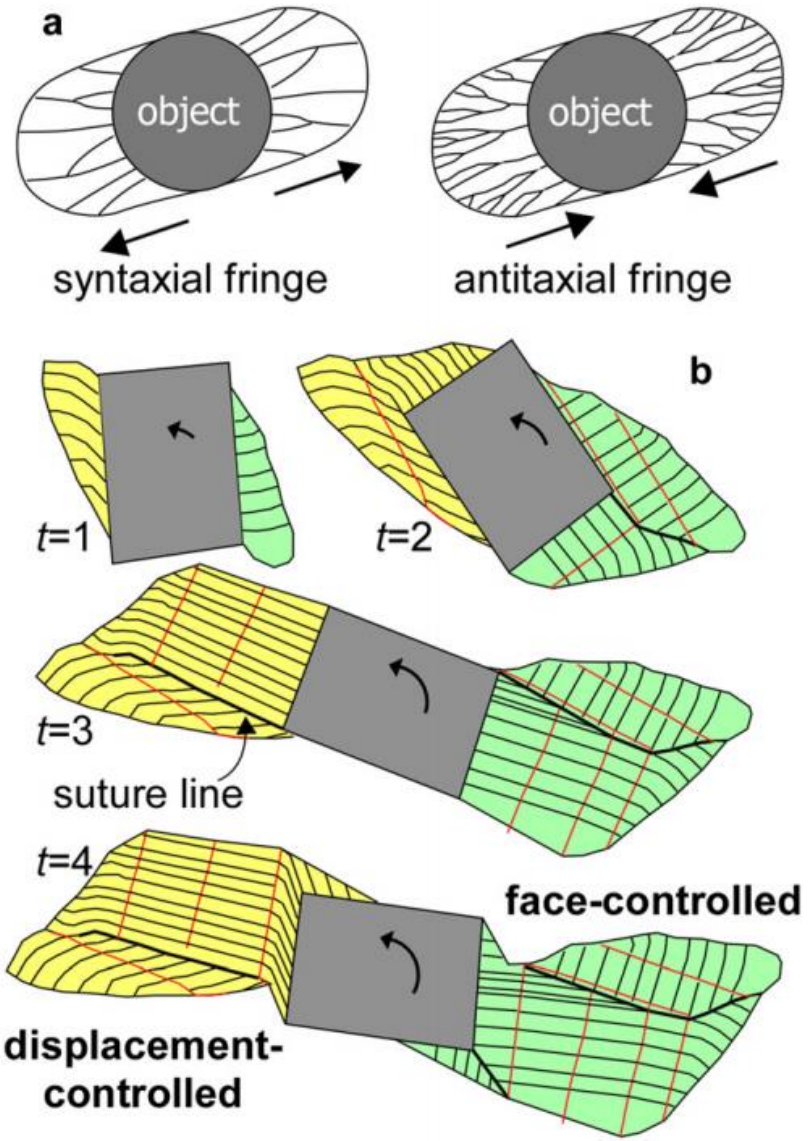

Bons et al., 2012

Folds after Pure Shear Deformation

Pure Shear

After 50% horizontal elongation under pure shear.

Original

After 50% add'tl horizontal shortening. (Pure shear)

Volume Constant Strain

From Marli Miller, U of Washington

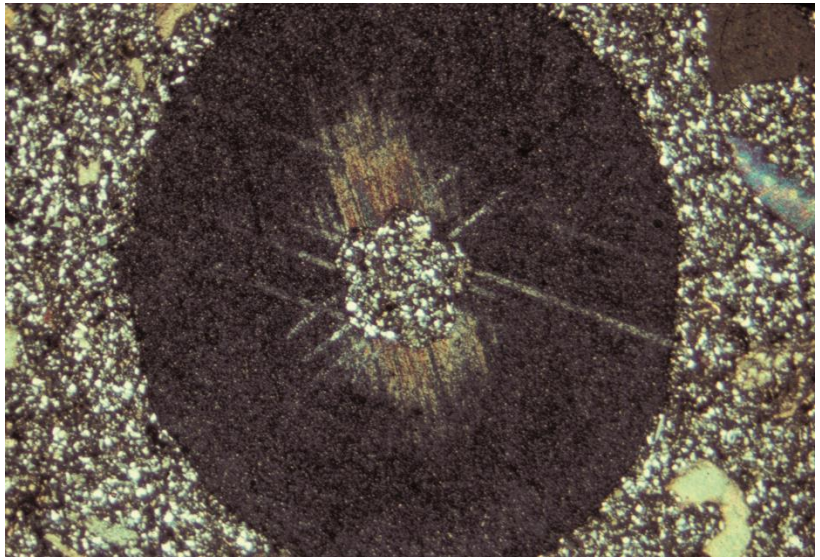

3.1.3 - Rheology

An AAPG Short Course by
Terry Engelder
Professor of Geosciences
The Pennsylvania State University

Ductile Deformation

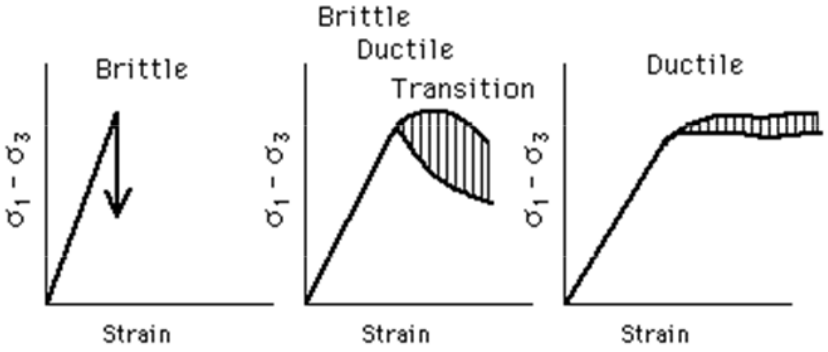

Ductile deformation occurs if the rock under stress does not loose its strength by means of a brittle failure. This behavior is illustrated using stress-strain curves from rock deformation experiments. Each test is run at constant strain rate which means that in a triaxial test the piston is advanced into the cylindrical rock sample at a constant rate. The initial behavior of the rock is elastic for which a linear stress-strain curve is shown. Brittle failure causes a complete lose of strength. Ductile flow shows that the strength is maintained during continuous straining of the sample.

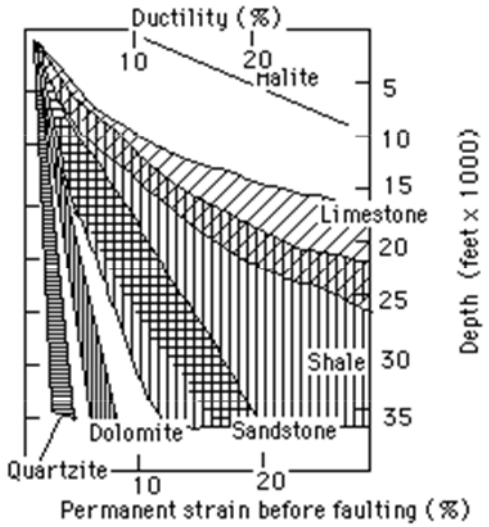

Percent ductility is a measure of the amount of strain that a rock undergoes before losing strength. Ductility varies with lithology. The strongest and most brittle of the rocks is a quartzite or silica cemented sandstone. In contrast, halite is very weak and will undergo large amounts of ductile flow without brittle failure. There is a variety of rocks and their relative ductilities as a function of depth of burial within the earth. Starting with the most brittle there is silica cemented sandstone, dolomite, calcite-cemented sandstone, shale, limestone, and halite.

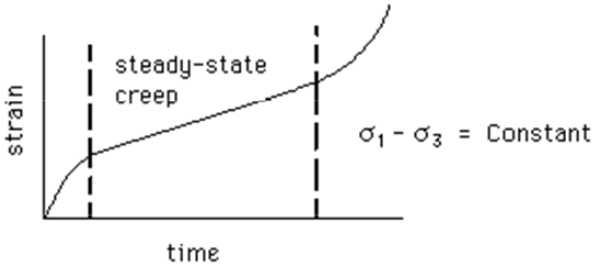

Initially constant strain-rate tests were most convenient for laboratory experiments. However, conditions within the crust of the earth closely resemble constant stress tests. This is so because the differential stress within the crust does not change rapidly with time. The most interesting characteristic of constant stress tests is that steady state creep is achieved. This is a state where the rock exhibits no change of strain rate with time.

Terry Engelder

Ductile Deformation

Various mechanisms of ductile flow were introduced during the previous lecture. Each of these mechanisms can be dominate during the creep of rocks. The dominate mechanism depends on the temperature and differential stress affecting the rock. For plotting the temperature of deformation verses stress, the temperature T is normalized to the melting temperature (T_m) by the ratio T/T_m. The stress of deformation is normalized by the shear modulus of the rock (μ).

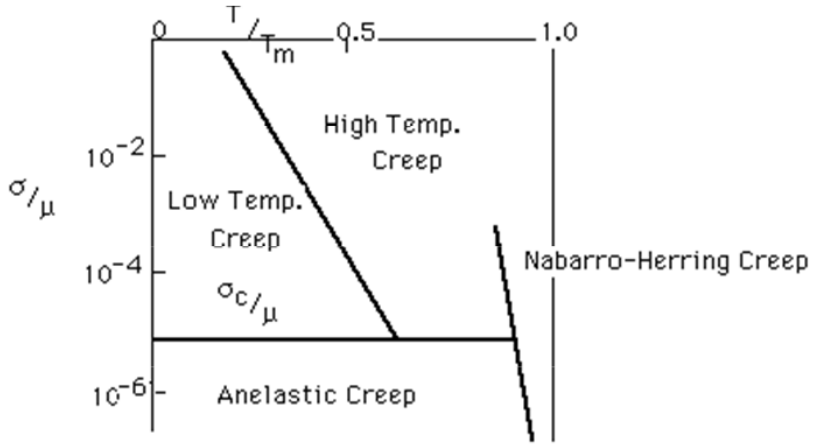

Various creep mechanisms include the following:

Nabarro-Herring Creep - bulk diffusion of point vacancies down a stress gradient. Recall that a point vacancy is a single missing atom.

Anelastic Creep - below a critical shearing stress for large dislocation movement mechanisms as Coble Creep take place.

Low-Temperature Creep - includes multiplication and glide of dislocations. Stresses have to be reasonably high to cause this type of creep.

High-Temperature Creep - at higher temperatures edge dislocations can climb and screw dislocations can cross slip.

An equation for Nabarro-Herring Creep gives the strain rate (é) in terms of stress σ

$$\acute{e} = (\alpha D V_a \sigma)/kTL^2.$$

α is a geometric factor; L is the diameter of the grain; D is the diffusion coefficient; V_a is the atomic volume; T is the temperature; σ is stress; and k is the Boltzman number. Here strain rate is proportional to stress which is the behavior of a Newtonian viscosity.

Terry Engelder

Steady State Creep

Steady creep flow of rock materials can also be modeled using the Weertman Equation

$$\dot{\varepsilon} = A\exp(-Q_c/RT)\, f(\sigma)$$

where T = temperature, Q_c = creep activation energy, and R = gas constant. This equation can be evaluated using a plot of log σ versus -log ($\dot{\varepsilon}$) by rearranging the above equation

$$\log(\dot{\varepsilon}/A) = Q_c/RT + \phi\log\sigma$$

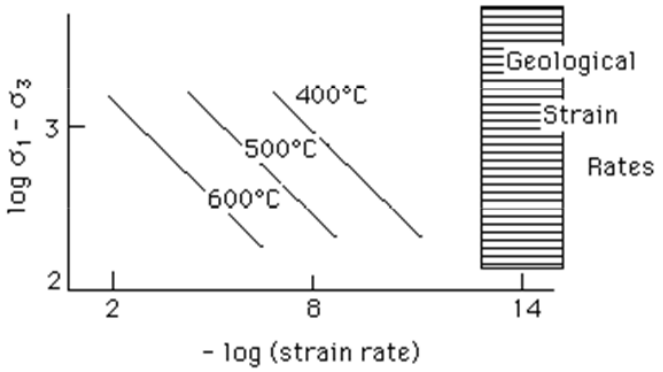

where ϕ is the slope of the lines in the plot to the left and Qc is determined as the slope of the plot of log $\dot{\varepsilon}$ versus 1/T at constant stress. Experiments show that creep rate at high temperature is a strong function of stress.

$$\dot{\varepsilon} = \alpha\sigma^{n}$$

The plot to the right is a deformation mechanisms map for calcite (limestone). Given a stress and temperature, the deformation mechanism diagram shows which of six mechanisms are favored. These mechanisms include cataclasis, pressure solution, dislocation glide, dislocation climb, Coble creep, and Nabarro-Herring creep

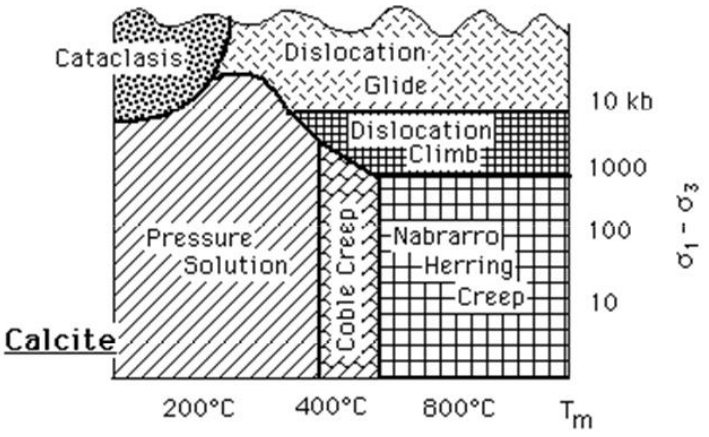

Terry Engelder

Intracrystalline deformation mechanisms

During a systematic investigation of the strength of rocks, focusing largely on ductile behavior, a critical step occurred when F. J. Turner (1948) hypothesized that twin lamellae in calcite or deformation lamellae in quartz originated by plastic flow and formed when the slip systems were in orientations of high shear stress. The study of rock strength narrowed to focus on the experimental deformation of marble largely because calcite is ductile under a wide range of experimental conditions.

Two distinct intracrystalline slip mechanisms are evident in petrographic thin sections of deformed rocks. These mechanisms, translation gliding and twin gliding, are controlled by crystallographic structures and represent the motion of dislocations (missing atoms in the atomic lattiace). Both mechanisms obey *Schmid' s law* which states that an intracrystalline slip mechanism will operate only when the shear stress resolved along the slip direction in the slip plane has reached a certain critical value (τ_c). Although τ_c is a function of temperature and strain rate, it is independent of the stress normal to the active slip plane, a very important observation because slip is an indication of a specific σ_d.

Twin gliding in calcite along with pressure solution of both quartz and calcite are the primary ductile deformation mechanisms in the brittle portion of the crust, the schizosphere.

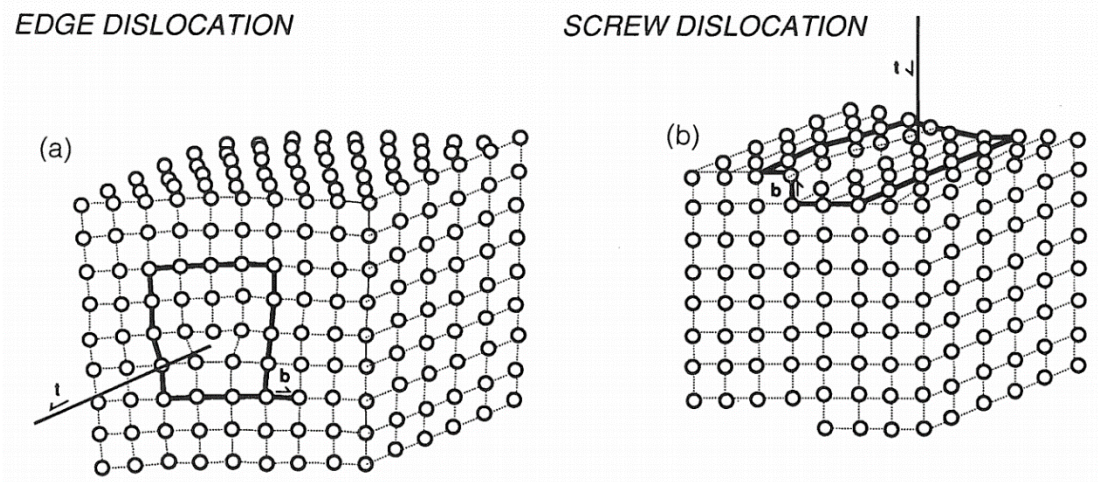

Schematic block diagrams of an edge dislocation and a screw dislocation in cubic lattices. The Burger's vector, **b,** is defined as the closure vector (the direction of motion) for the loop counted around the dislocation (dark line). The tangent vector, **t,** is defined to lie parallel to the dislocation line. The Burger's and tangent vectors are perpendicular for an edge dislocation; in contrast, they are parallel for a screw dislocation.

Terry Engelder

Translation gliding is the macroscopic manifestation of edge dislocation motion along a slip plane. The large-scale effect of translation gliding is the deformation of the host grain in simple shear with each atomic plane displaced an integral atomic distance relative to the plane. Displacement along any slip plane is limited by crystallographic symmetry to one or a few slip directions with the slip plane and slip direction comprising a *slip system.* Crystals may have more than one slip system, each with a unique τ_c. The slip system with the lowest τ_c is the most active system. The resolved shear stress (τ_r) along a given slip direction is given by

$$\tau_r = (\sigma_1 - \sigma_3)\Omega_o \quad \text{and} \quad \Omega_o = \cos\lambda\cos\phi$$

where λ is the angle between σ_1 and the normal to the slip plane and ϕ is the angle between σ_1 and the slip direction. The maximum τ_c occurs on a slip system where $\lambda = \phi = 45°$ so that $\Omega_0 = 0.5$. Slip will occur only if $\tau_r \geq \tau_c$. However, for homogeneous deformation of an aggregate, five slip systems must operate, an observation called the von Mises criterion.

Although *twin gliding* is also regarded as a simple shear of the crystalline lattice along the slip plane, it differs from translation gliding in two respects. First, it is homogeneous which means that each lattice plane is displaced the same amount relative to the plane below. There are no such constraints on the motion of each lattice plane during translation gliding. Secondly, the twinned portion of a crystal is deformed into a mirror image of the undeformed crystalline lattice across the twin plane.

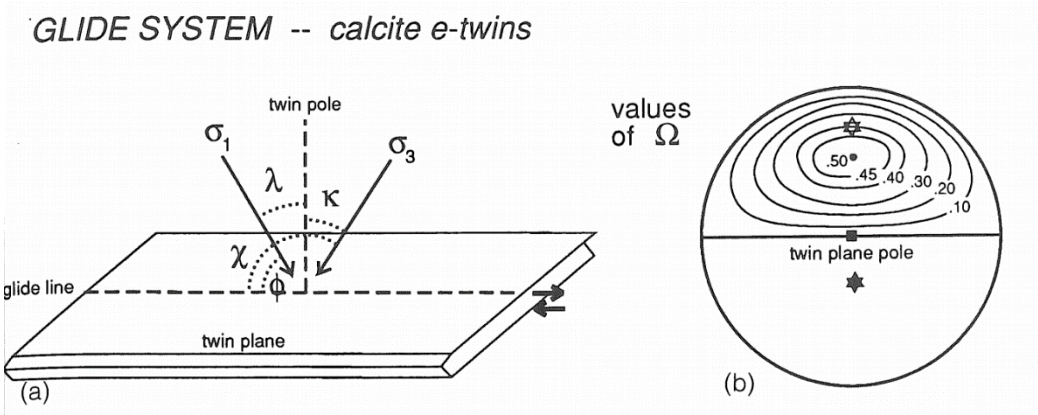

Diagram showing the nature of the gliding system tor calcite e-twins relative to principal stress axes and angles given here. (b) Contoured values of Ω_0 for a horizontal twin plane (after Jamison and Spang, 1976)

Terry Engelder

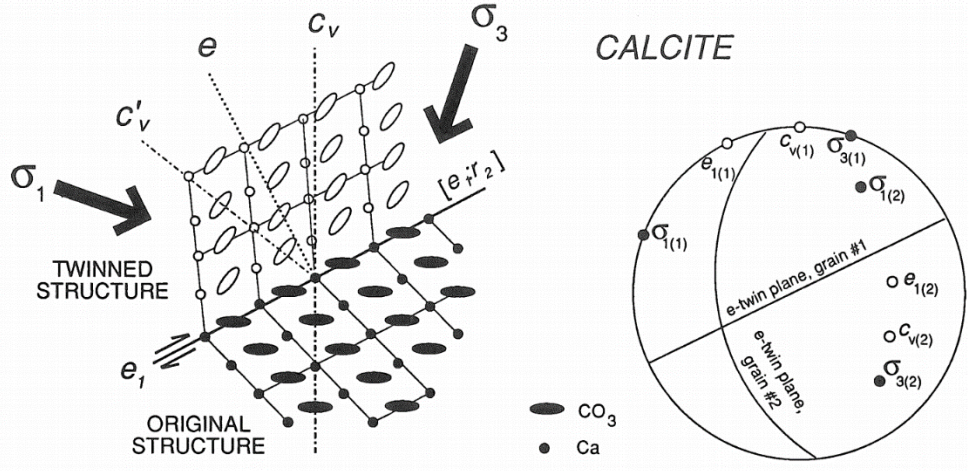

Twin-gliding in calcite. Diagrammatic projection of the twinned calcite structure parallel to the plane containing the c-axis and the normal to σ_1, showing the twinning elements (adapted from Friedman, 1964). Equal-area projection showing the graphic method for constructing principal stress axes best oriented to produce twin gliding in calcite for two e-planes (adapted from Carter and Raleigh, 1969).

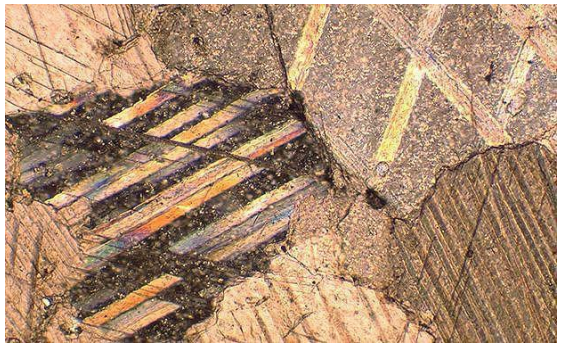

Calcite twinning is one of the key deformation mechanisms used in the study of stress during ductile flow in the schizosphere. For twinning on the e-planes, the atomic layers above the twin plane move toward the c-axis in the host crystal with respect to the atomic layers below the twin plane. Here is a micrograph of calcite twin lamallea in a deformed marble.

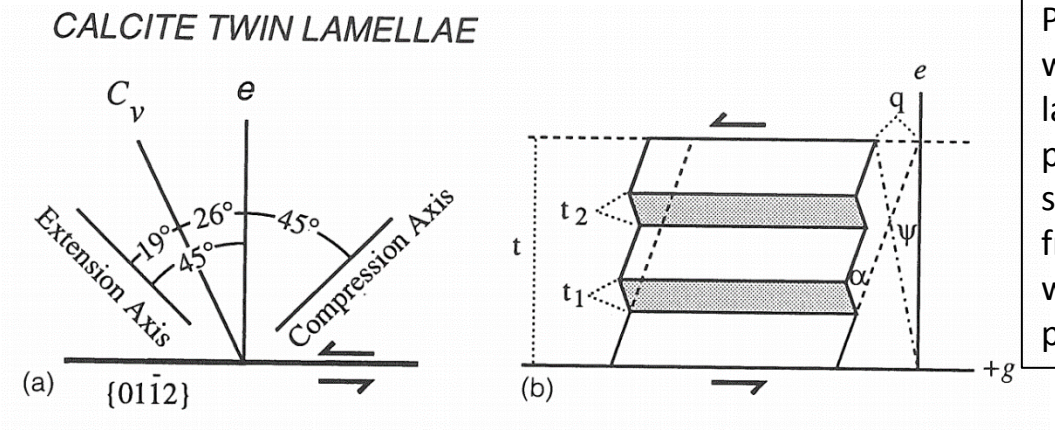

Position of compression and extension axes that would most favor development of calcite twin lamellae where plane of diagram is normal to e-twin plane and contains glide direction [e1:r2]. (b) Shear strain in a partially twinned calcite grain (adapted from Groshong, 1972). The values t_1 and t_2 are the widths of twins and tis the width of the host grain perpendicular to the twin planes.

Engelder, 1993

Intergranular Mechanisms: Pressure solution
Pebble Conglomerate, Beavertail Point, Rhode Island, USA

Ductile deformation mechanisms alone or combined with other mechanisms act to facilitate the changes in the shape of rocks at various levels in the crust of the earth. The higher the temperature (i.e. the deeper within the crust), the more likely that ductile mechanisms dominate over brittle mechanisms in controlling the style of deformation. Ductile mechanisms caRn be divided into intergranular and intragranular processes. Higher temperatures favor intragranular processes.

Near the surface of the crust pressure solution is the most common intergranular deformation mechanism. It is manifested by cleavage in sedimentary rocks. The basic process involves a dissolution at contact points between grains of rock. Characteristically one grain will dissolve faster than the other. The product of this differential dissolution is a stylolite in fine-grained rocks or pits and beards in pebbles of a conglomerate. The dissolution process is believed to be activated by the high normal stress between grain contacts. The rock, dissolved from the high stress contacts, then diffuses into the pore spaces of the rock where pore fluid exerts the only normal stress at pressures much less than found along grain-to-grain contacts.

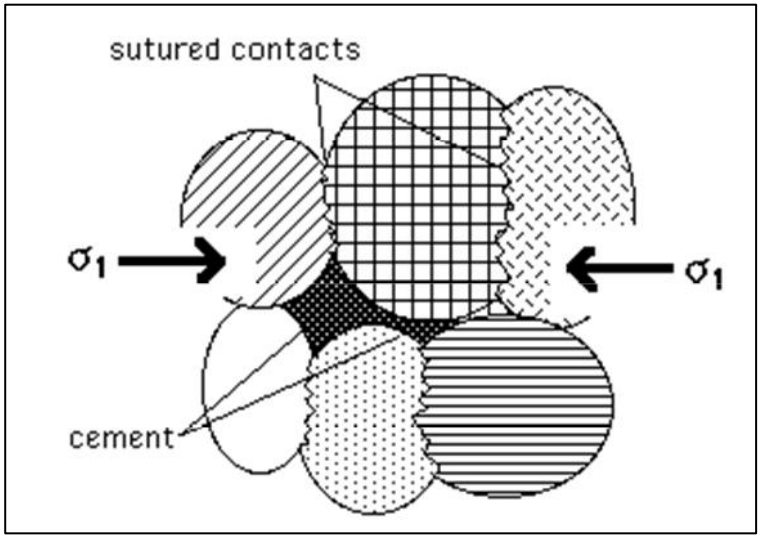

In two or more component systems one material will dissolve faster than another. For example, in a pelagic limestone the calcite dissolves and clay forms as an insoluble residue. In a one component system, the single component dissolves uniformly. In a shale (clay) the composition of the shale after 50% shortening is the same as the initial shale. In quartzites the grain boundaries are irregular as the grains penetrate each other. The normal to the irregular surface that is the stylolite points in the direction of σ_1 acting on the rock. If the interpenetration is large enough, large protrusions of one material penetrates another material to point in the direction of σ_1.

Terry Engelder

The orientation of stylolites and pressure solution cleavage is always consistent relative to σ_1. The maximum rate of dissolution is in the direction along a surface normal to σ_1. This favors the formation of a cleavage with its "planar" direction normal to σ_1 and σ_1 may be either vertical or horizontal.

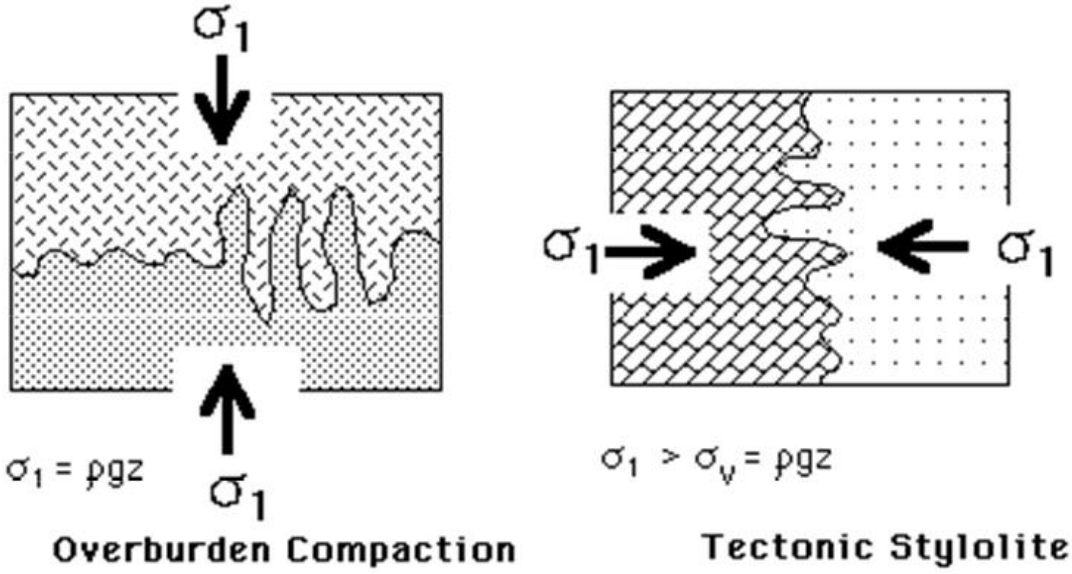

Terry Engelder

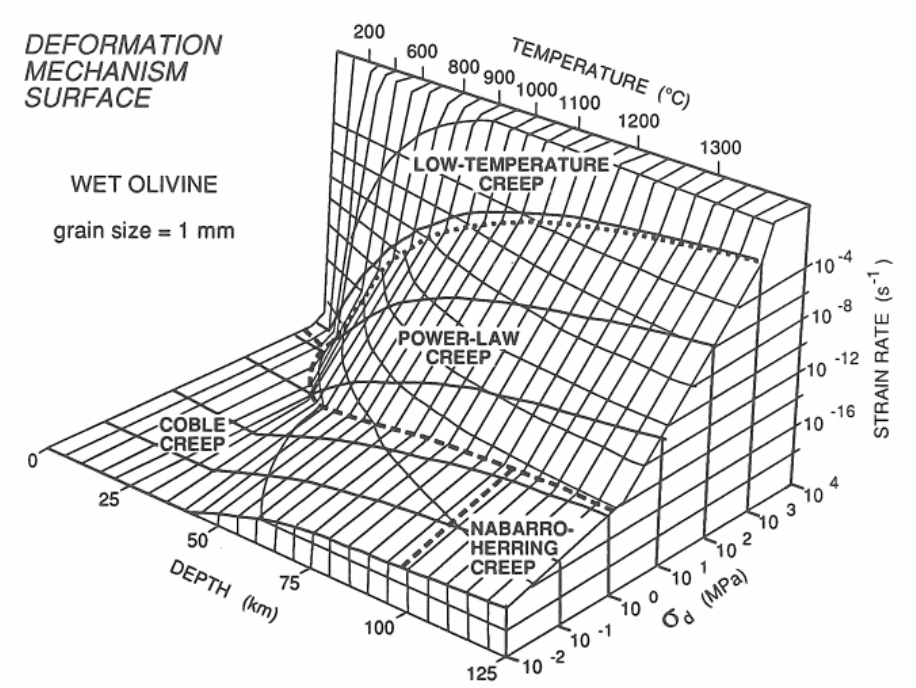

Deformation mechanism surface showing flow regimes and processes for wet olivine (adapted from Tsenn and Carter, 1987).

Different flow laws describe the behavior of rocks when different deformation mechanisms are rate controlling. Various flow regimes are identified with subdivisions of a temperature-ε(rate)-σ_d plot known as a *deformation mechanism map* (Stocker and Ashby, 1973). In the **upper tier** of the ductile-flow regime, grain-size-sensitive creep mechanisms are important. Three grain-size mechanisms include diffusional flow, pressure solution, and superplastic flow (e.g., Durney, 1972; Schmid, 1983). The **middle tier** of the ductile-flow regime is characterized by low-temperature creep for which flow stress is relatively insensitive to temperature and strain-rate changes (Kirby, 1980). Here dislocation glide dominates and dislocation pile-up leads to failure which may be brittle. In the high temperature creep *(power-law creep)* regime (**lower tier**), relatively small temperature changes have a marked effect on the steady-state flow stress, cr; (Kirby, 1983).

Terry Engelder

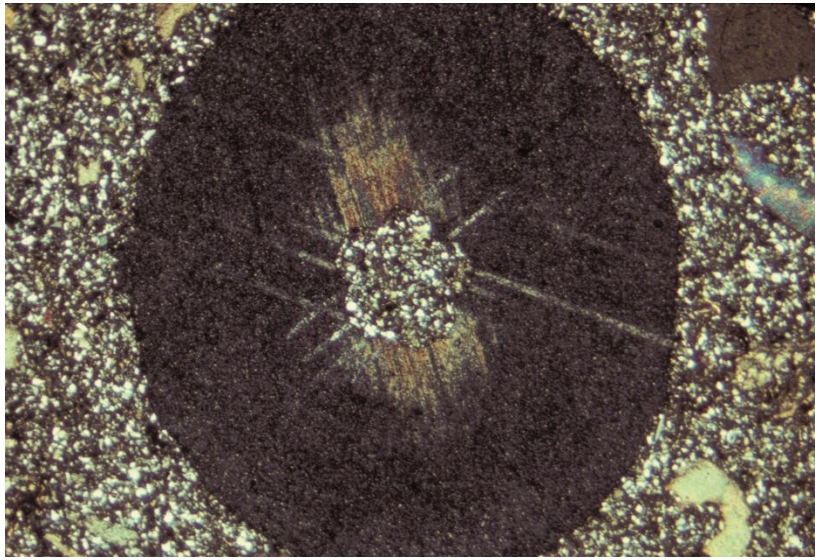

3.1.4 – Plastosphere v. Schizosphere

An AAPG Short Course by
Terry Engelder
Professor of Geosciences
The Pennsylvania State University

Schizosphere versus Plastosphere

Constraints on lithospheric stress are based on ductile as well as brittle rock strength. Temperature and confining pressure have fundamentally different effects on brittle and ductile rock strength. Ductile strength is almost unaffected by confining pressure, whereas the brittle strength of rock increases markedly at higher confining pressure (Heard, 1960). In contrast, temperature has a large effect on ductile processes such as dislocation motion and diffusion-assisted deformation, whereas brittle strength shows little dependence on temperature (Heard, 1963). In laboratory experiments, rocks are markedly weaker during ductile deformation at high temperature which means that σ_d is much lower in the warmer portions of the **plastosphere** and in regions of the **schizosphere** dominated by ductile deformation. Semibrittle behavior occurs in the transition from pressure-dominated brittle deformation to temperature-dominated ductile deformation (Tullis and Yund, 1977). Semibrittle behavior is found in a transition zone of the lithosphere where cr, gradually drops from a maximum at depths of 10-15 km to smaller values at depths near the Moho. This brittle-ductile transition zone is the boundary between the schizosphere and plastosphere. The Moho apparently represents a mechanical discontinuity within the lithosphere where the underlying peridotite is stronger than rocks of the lower crust (Kirby, 1985). As is the case with the lower crust, strength of the mantle drops as temperature increases with depth.

Engelder, 1993

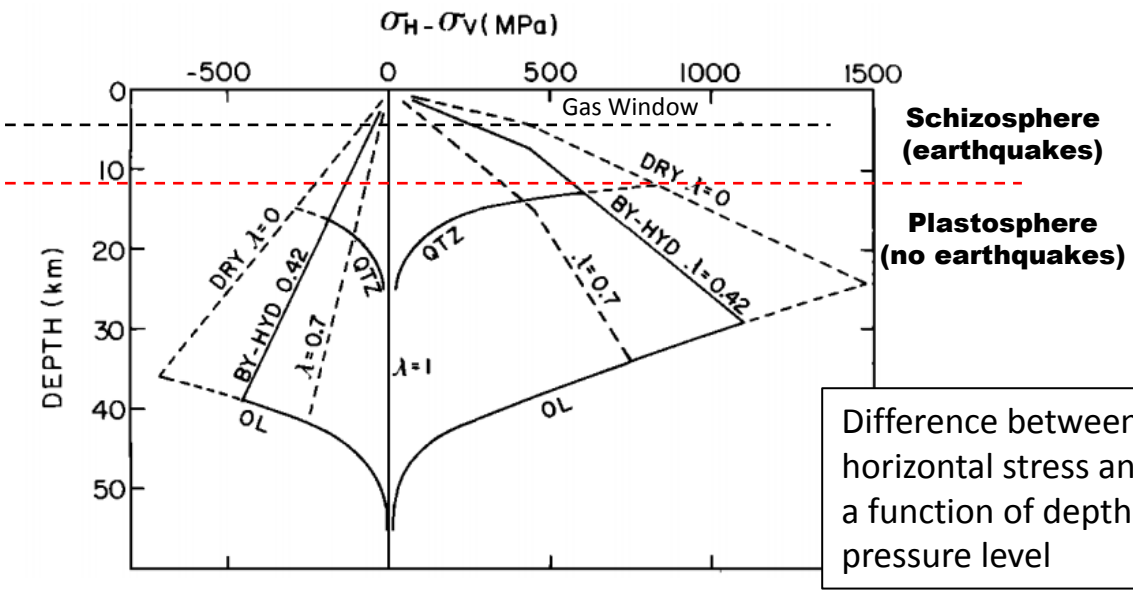

The limits within which lithospheric stress must lie on the basis of the assumptions (1) that rocks are fractured and that friction on fractures controls the stress at shallow depths,(2) that the creep properties of quartz or olivine control the stress below about 15 or 25 km, respectively, and (3) that the effective stress principle operates for friction but not for creep.

Difference between maximum or minimum horizontal stress and the vertical stress as a function of depth. Values of λ give pore pressure level

Brace & Kohlstedt, 1980

Stress Regimes in the Lithosphere

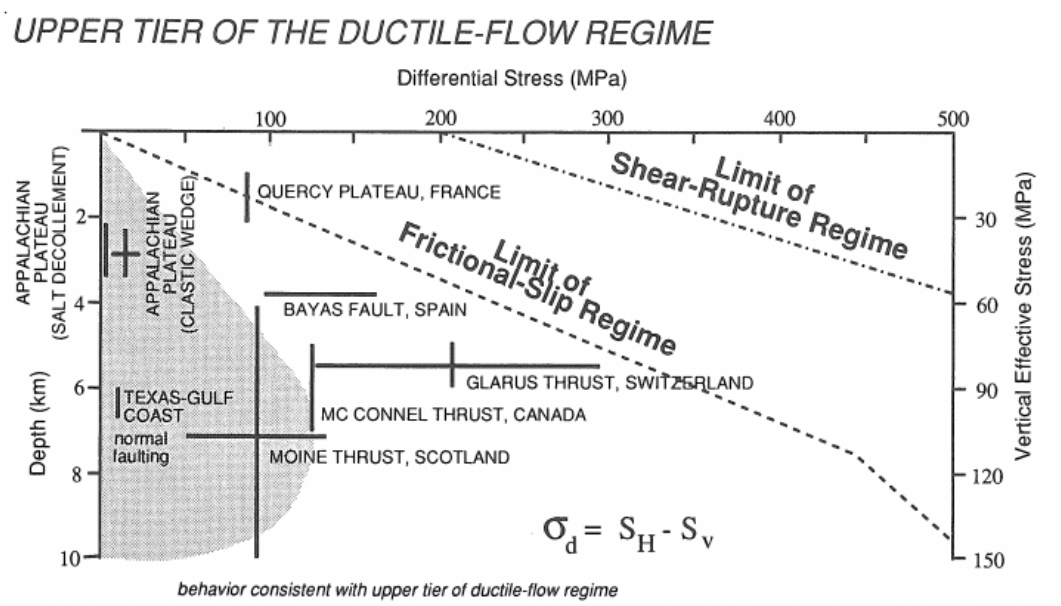

Plot of σ_d versus depth within the upper tier of the ductile-flow regime. Data from Carter et al. (1982); Blenkinsop and Drury (1990); Engelder (1982); Friedman and Heard (1974); Jamison and Spang (1976); Kappmeyer and Wiltschko (1984); Pfiffner (1982); Tourneret and Laurent (1990); and Twiss (1977).

A compilation of data from the upper tier of the ductile-flow regime reveals that while σ_d near fault zones approaches the frictional strength of the schizosphere (i.e., Zoback 2007), there is plenty of evidence indicating that the heart of foreland fold-thrust belts was generally at σ_d, much less than required for frictional slip. Data from the Glarus Thrust in Switzerland indicate that σ_d was near the frictional strength of the upper crust (Briegel and Goetze, 1978). Within the Marquette Synclinorium, Michigan, σ_d varied from 1 to 36 MPa (Kappmeyer and Wiltschko, 1984). σ_d near other major faults was lower, ranging from 125 MPa near the McConnell Thrust of the Canadian Rockies to 2.5 MPa along the Appalachian Plateau decollement. Fold-thrust belts riding atop a salt decollement (e.g., the Appalachian Plateau, the Franklin Mountains of Canada, the Jura of the Alps) are extremely wide and characterized by a small cross-sectional taper angle (Davis and Engelder, 1985). The width of these fold-thrust belts is attributed to the extremely weak nature of the salt decollement and a relatively low σ_d within the elastic wedges. All of this means that earthquakes, a frictional phenomenon responding to higher σ_d are not common within the elastic wedges of fold-thrust belts in the schizosphere and that ductile flow at relatively low σ_d plays a major role in foreland deformation (Groshong, 1988).

Engelder, 1993

Upper tier of the ductile flow regime

If σ_d was too low for brittle frictional slip during certain phases of mountain building, what is the explanation of the pervasive faults throughout forelands? Part of the explanation is tied to the nature of faulting which is characterized by slickensides coated with secondary mineral growth. The *slickenlines* on these surfaces are not brittle wear grooves indicative of high frictional stresses but rather fibrous minerals indicative of local dissolution and mineral growth. Technically, slip by a ductile mechanism is also frictional slip, however in the context of this book the frictional-slip regime refers to σ_d developed as a consequence of brittle wear. The Umbrian Apennine fold-thrust belt contains an array of faults displaying slickenlines. Such faults have a preferred orientation and fall into one of two clusters forming conjugate sets with a 90° dihedral angle (Marshak et al., 1982). A conjugate set of faults forming at a 90° dihedral angle is unusual for brittle behavior. A 90° dihedral angle suggests that the faults slipped at the maximum τ, a situation indicative of a ductile creep mechanism (i.e., stress solution) rather than a brittle friction. If so, these fault surfaces slipped under relatively low τ in the upper tier of the ductile-flow regime. In other mountain belts σ_d is sufficiently low so that the crack propagation under high pore pressure is the favored brittle deformation mechanism. During the Alleghanian Orogeny, not only was brittle deformation of elastic sediments of the Appalachian Plateau restricted to crack propagation (e.g., Babat and Engelder, 1984), but also the Alleghanian joints were not reactivated in frictional slip after the stress field rotation to subject early joints to τ (Geiser and Engelder, 1983). This further suggests that σ_d remained relatively low throughout large portions of the Appalachian Plateau.

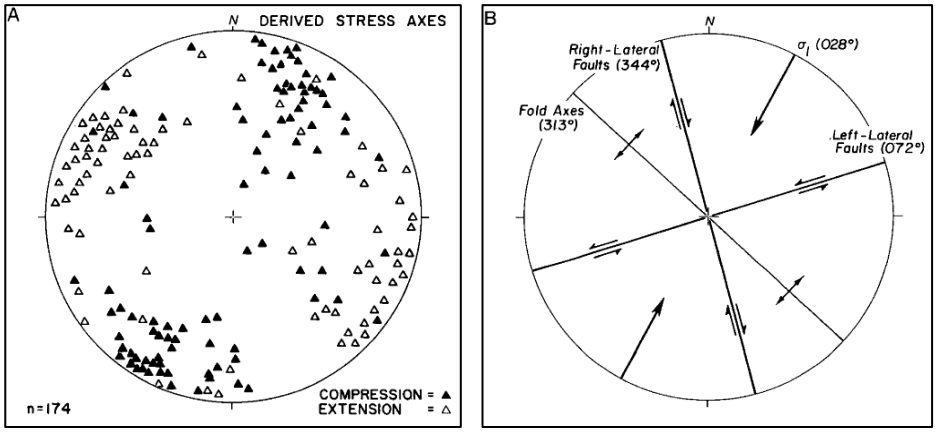

The strata of the northern Umbrian Apennine fold belt are cut by an array of mesoscopic faults that generally display strike- or oblique-slip offset. The majority of these faults have traces less than a few metres long and represent displacements of < I 0 cm. Fault surfaces are associated with stylolites and are coated with elongate calcite fibers, suggesting that movement occurred by the mechanism of pressure-solution slip. There is a great range among fault attitudes, but two clusters forming a conjugate set with about a 90° dihedral angle stand out (Marshak et al., 1982).

Engelder, 1993

Middle tier of the ductile flow regime

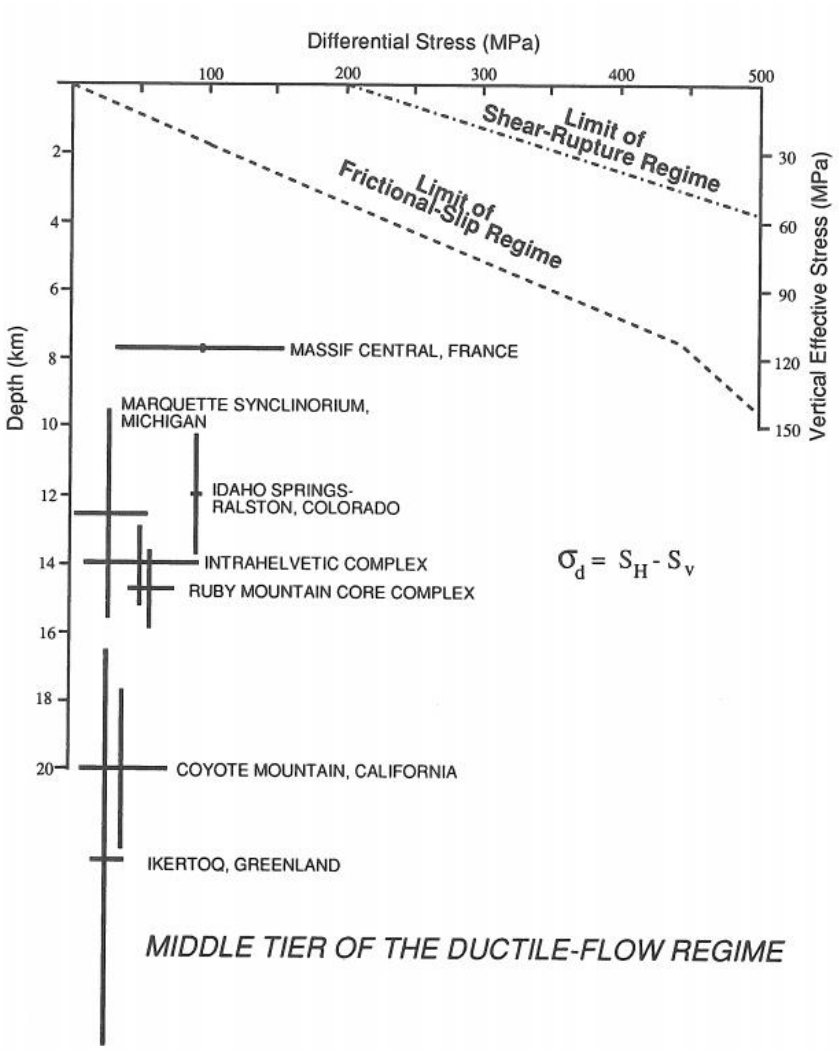

Stress in the middle tier of the ductile-flow regime is largely known from fault zones in quartz-bearing rocks σ_d ranges from as low as 20-40 MPa along the Ikertoq shear zone in Greenland (Kohlstedt et al., 1979) to as high as 130 MPa in the Massif Central of France (Burg and Laurent, 1978). Some of the fault zones come from depths as great as 30 km where temperatures range up to 800°C. Work on calcite from the Glarus mylonite and within the Intrahelvetic complex yield σ_d estimates of 25-260 MPa and 42- 100, respectively (Pfiffner, 1982). Although stresses as high as 200 MPa are reported for the Mullen Creek-Nash Fork shear zone in Wyoming (e.g., Weathers et al., 1979), these data are based on free dislocation density which is notoriously sensitive to late-stage stress changes. In some fault-zone samples, a low Pdis or large recrystallization grain size may reflect a statically annealed state associated with stresses generated during uplift, erosion, and cooling (Kohlstedt and Weathers, 1980). Samples from the Ikertoq shear zone, for example, indicate a relatively low *a,* which, Kohlstedt and Weathers (1980) suggest, does not represent the major episode of deformation within the fault zone but rather some other point in a complicated history during uplift and erosion.

Engelder, 1993

Lower tier of the ductile flow regime

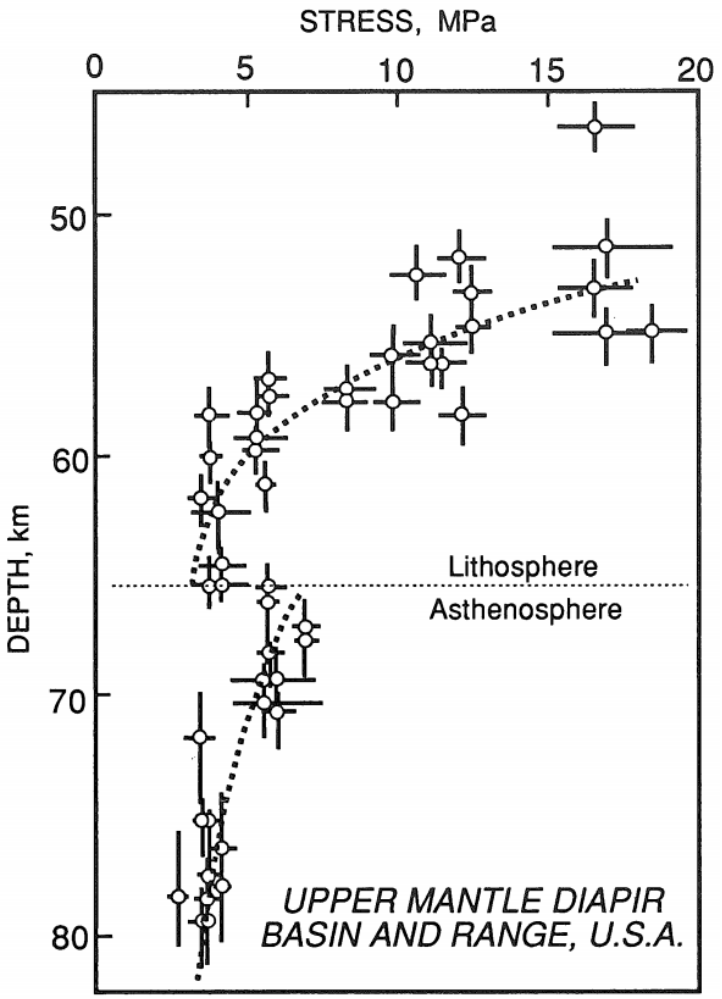

Estimates for σ_d in the Basin and Range of the United States using recrystallization grain size (adapted from Mercier, 1980). Estimates are obtained by using Ross's et al. (1980) grain boundary migration piezometer. These data are characteristic of the stress-depth trend for the lower tier of the ductile-flow regime.

The ductile-flow regime within the lithosphere has three tiers which correspond to the schizosphere, the brittle-ductile transition, and the plastosphere. Within all three tiers ductile flow serves to modulate σ_d which otherwise would climb until the point of inducing either frictional slip or shear rupture. From the **upper to lower tiers, the dominant deformation mechanisms are diffusion mass** transfer, restricted dislocation glide, and dislocation creep, respectively. The upper tier of the ductile-flow regime is found in that portion of the lithosphere characterized by the three brittle-stress regimes. In foreland settings there is apparently a symbiosis between the upper tier of the ductile-flow regime and the crack-propagation regime such that ductile flow suppresses σ_d to favor crack propagation upon increase in P_p above hydrostatic pressure. In a sense, the upper tier of the ductile-flow regime can occupy the same space as the frictional-slip or shear-rupture regimes, but the ductile-flow and high-stress regimes do not occupy that space concurrently. In the middle and lower tiers of the ductile-flow regime, brittle deformation is suppressed by high confining pressure in favor of dislocation glide (slip, twinning), dislocation creep (climb, cross-slip), and other high-temperature diffusion mechanisms.

Engelder, 1993

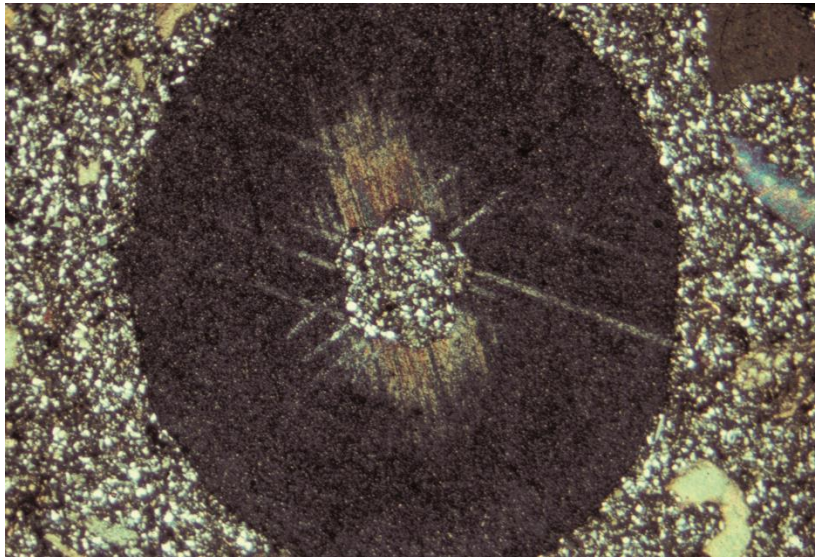

3.1.5 – Ductile Shear Zones

An AAPG Short Course by
Terry Engelder
Professor of Geosciences
The Pennsylvania State University

Conceptual Model of a Major Fault Zone

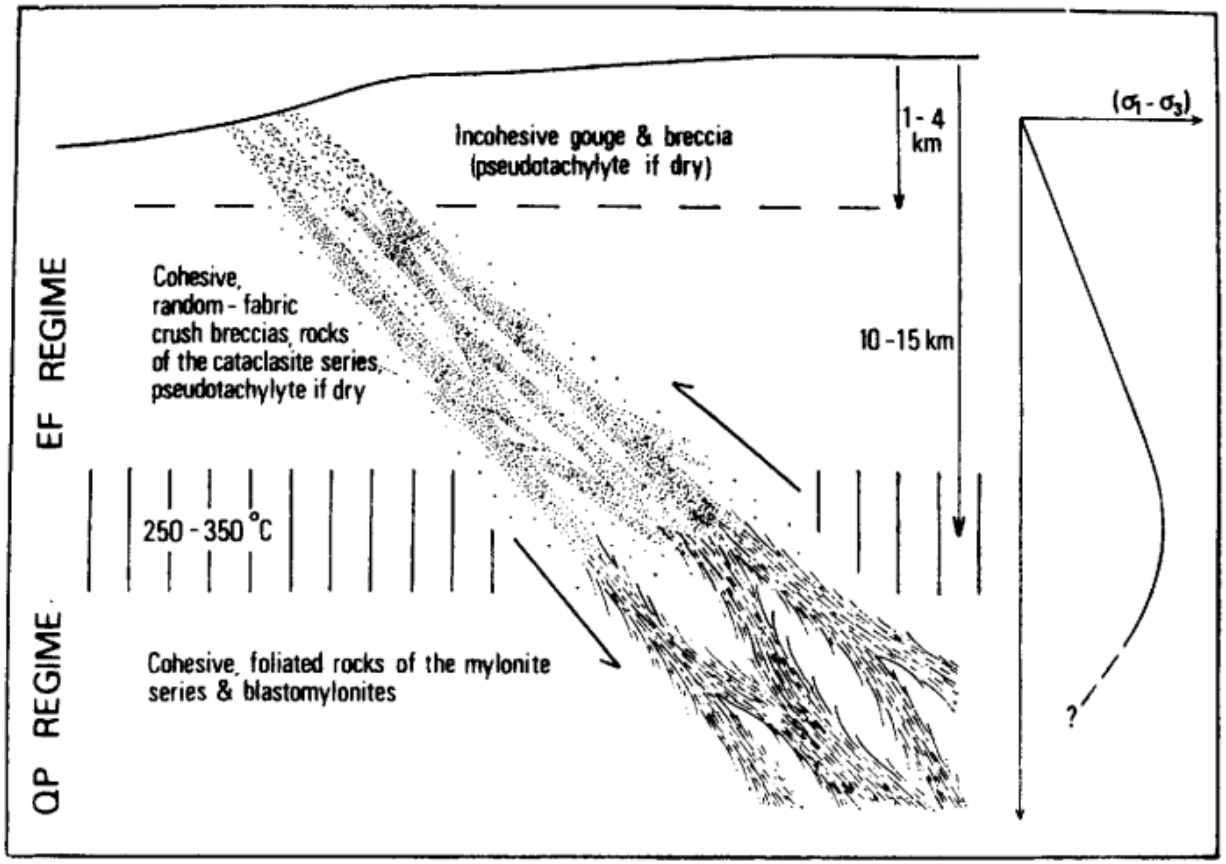

*Physical factors likely to affect the genesis of the various fault rocks--frictional properties, temperature, effective stress normal to the fault and differential stress--are examined in relation to the energy budget of fault zones, the main velocity modes of faulting and the type of faulting, whether thrust, wrench, or normal. In a conceptual model of a major fault zone cutting crystalline quartzo-feldspathic crust, a zone of elastico-frictional (EF) behaviour generating random-fabric fault rocks (gouge--breccia-- cataclasite series--pseudotachylyte) overlies a region where quasi-plastic (QP) processes of rock deformation operate in ductile shear zones with the production of mylonite series rocks possessing strong tectonite fabrics. In some cases, fault rocks developed by transient seismic faulting can be distinguished from those generated **by** slow aseismic shear. Random-fabric fault rocks may form as a result of seismic faulting within the ductile shear zones from time to time, but tend to be obliterated by continued shearing. Resistance to shear within the fault zone reaches a peak value (greatest for thrusts and least for normal faults) around the EF/OP transition level, which for normal geothermal gradients and an adequate supply of water, occurs at depths of lO-15 km.*

Sibson, 1977

Incipient cataclasis

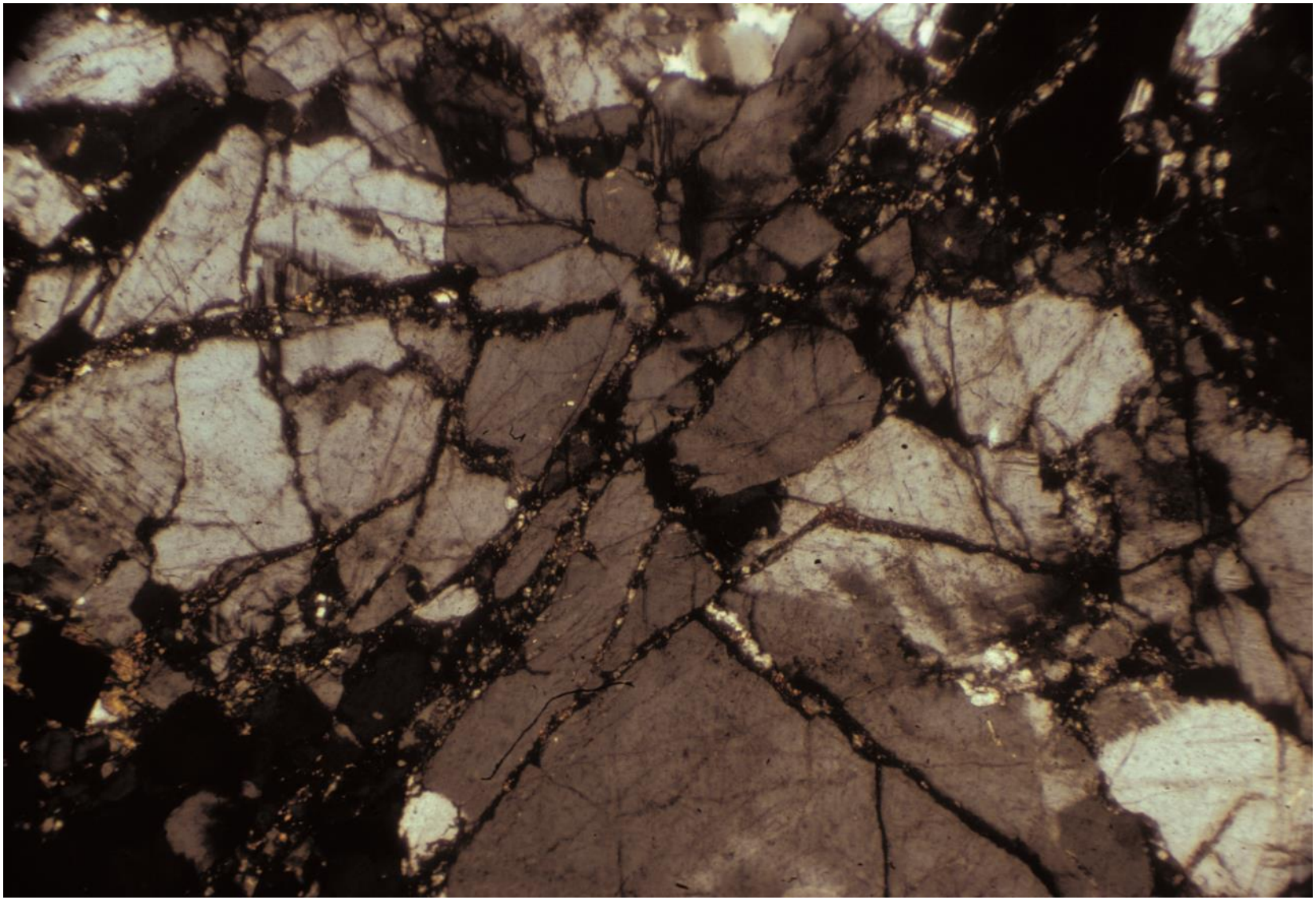

Terry Engelder

Cataclastic Shear Fractures
Cretaceous Sandstone, Bonita Fault, Tucumcari, New Mexico, USA

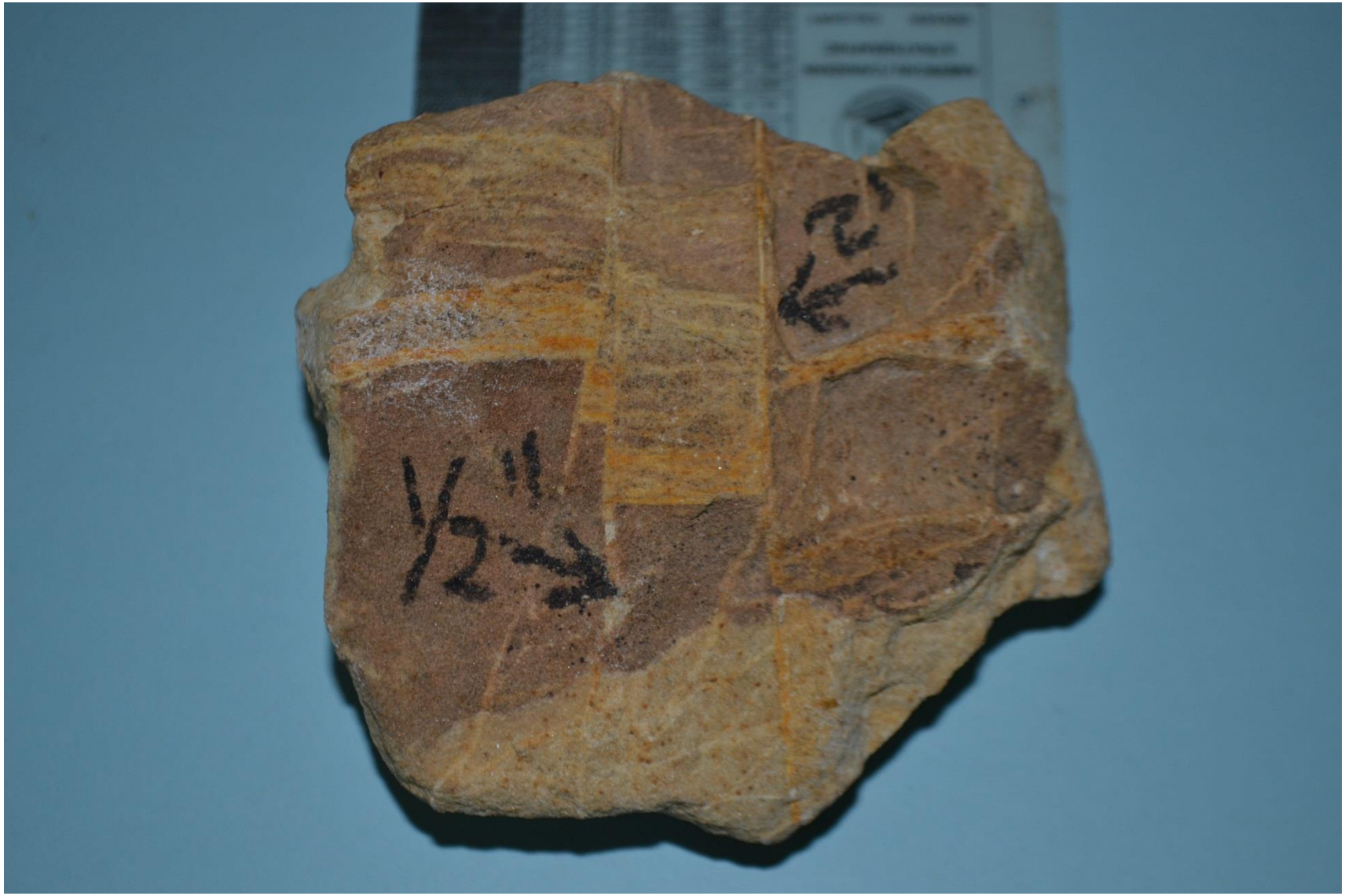

Terry Engelder

Cataclastic deformation band

Terry Engelder

Mylonites
Moine Thrust, Stack of Glencoul, Scotland, United Kingdom

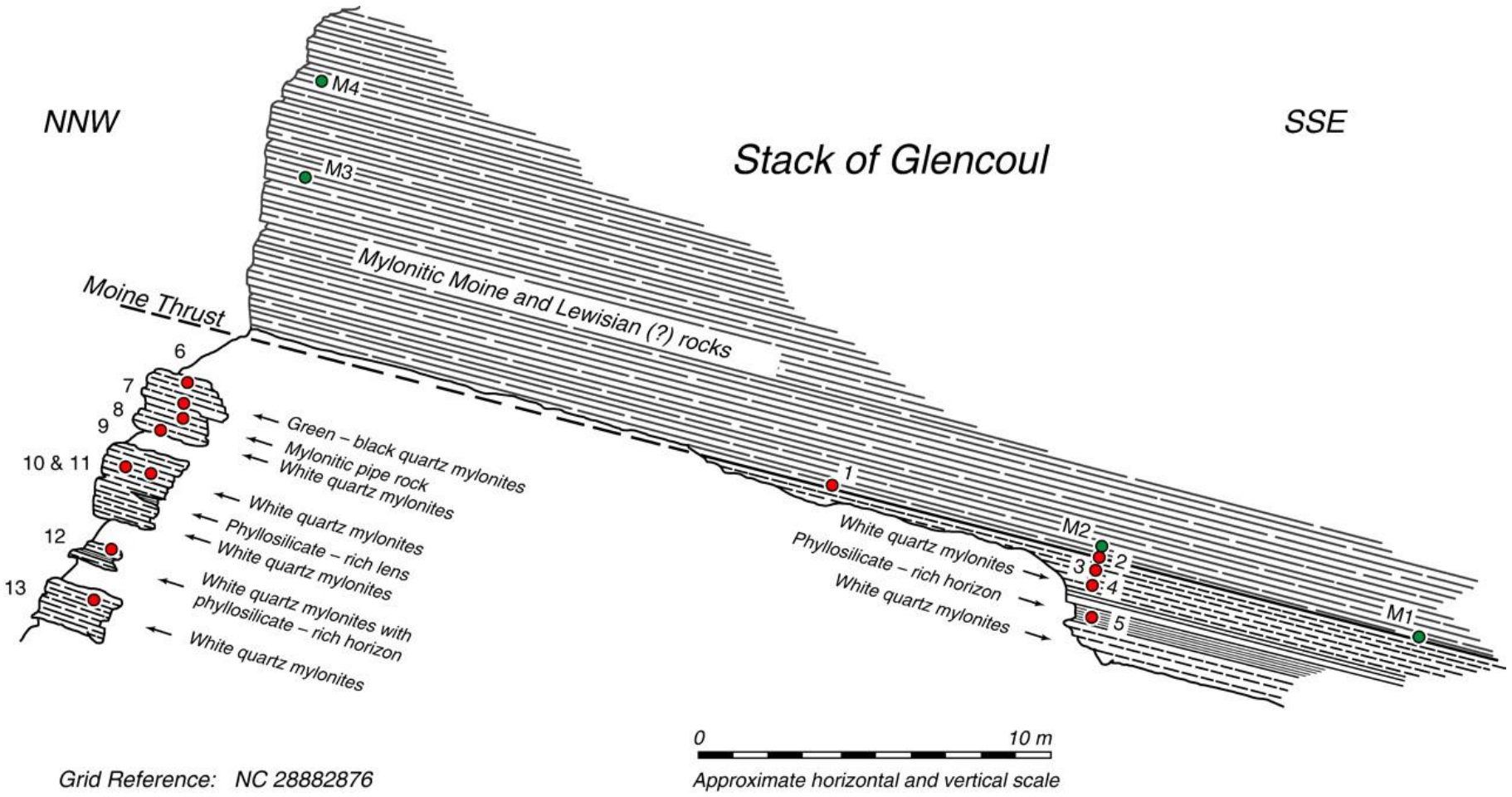

R.D. Law, 2010

Mylonites
Moine Thrust, Stack of Glencoul, Scotland, United Kingdom

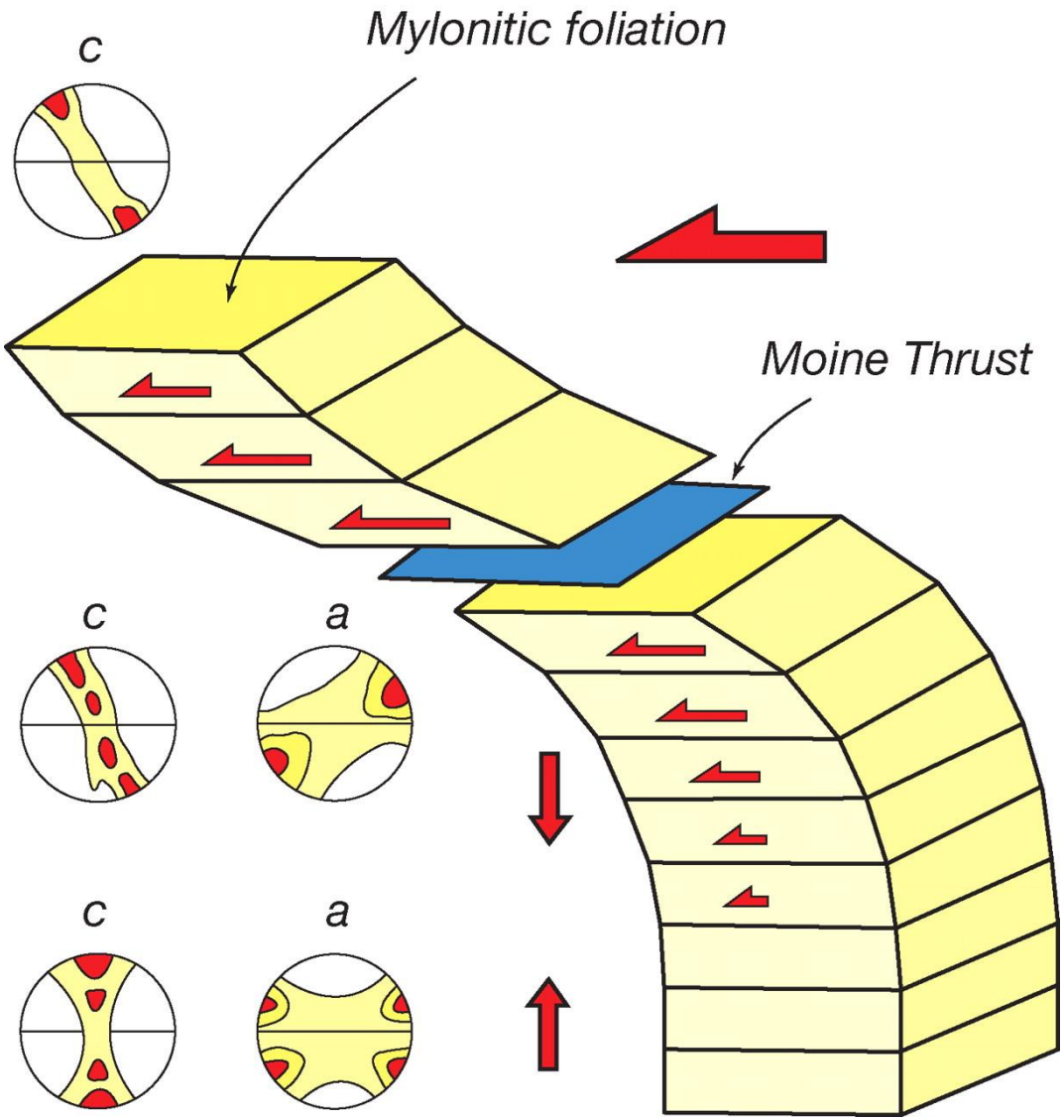

R.D. Law et al., 2010

Green-Black Mylonites
Moine Thrust, Stack of Glen Coule, Scotland, United Kingdom

Terry Engelder

White Quartz Mylonites
Moine Thrust, Stack of Glen Coule, Scotland, United Kingdom

Terry Engelder

White Quartz Mylonites
Moine Thrust, Stack of Glen Coule, Scotland, United Kingdom

Terry Engelder

Lewisian Rocks
Moine Thrust, Stack of Glen Coule, Scotland, United Kingdom

Terry Engelder

Lewisian Rocks
Moine Thrust, Stack of Glen Coule, Scotland, United Kingdom

Terry Engelder

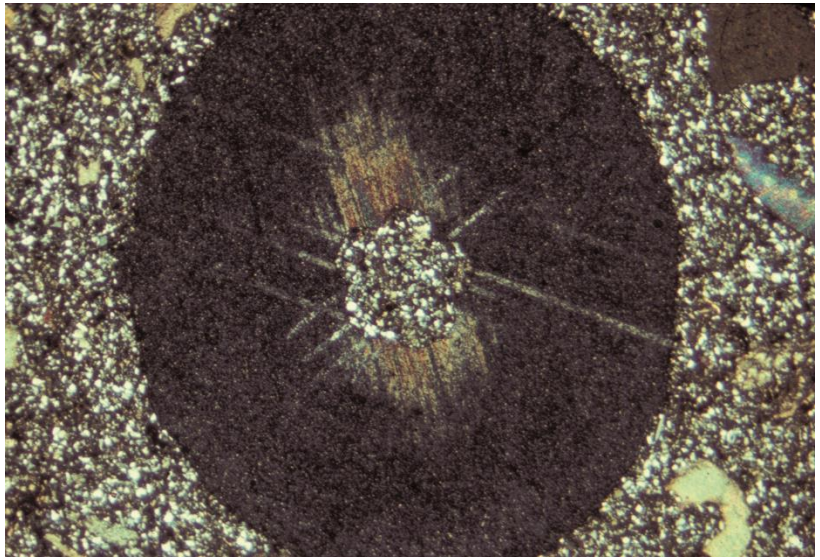

3.1.6 – Structures of the Plastosphere

An AAPG Short Course by
Terry Engelder
Professor of Geosciences
The Pennsylvania State University

Passive folding
Bronson Hill Anticlinorium, Massachusetts, USA

Terry Engelder

Bronson Hill Anticlinorium
Nappes and Gneiss Domes, Massachusetts, USA

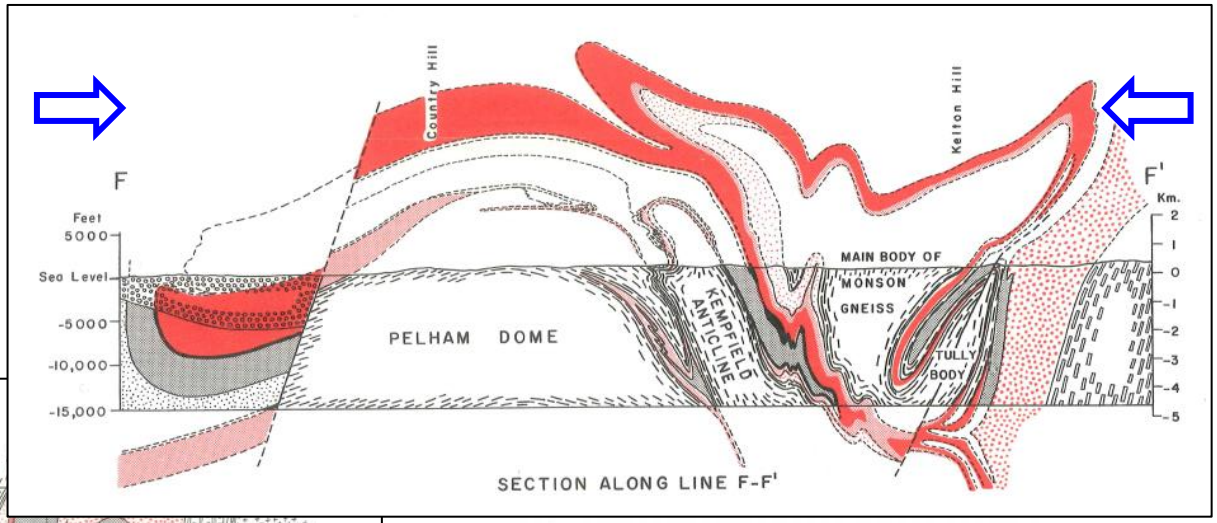

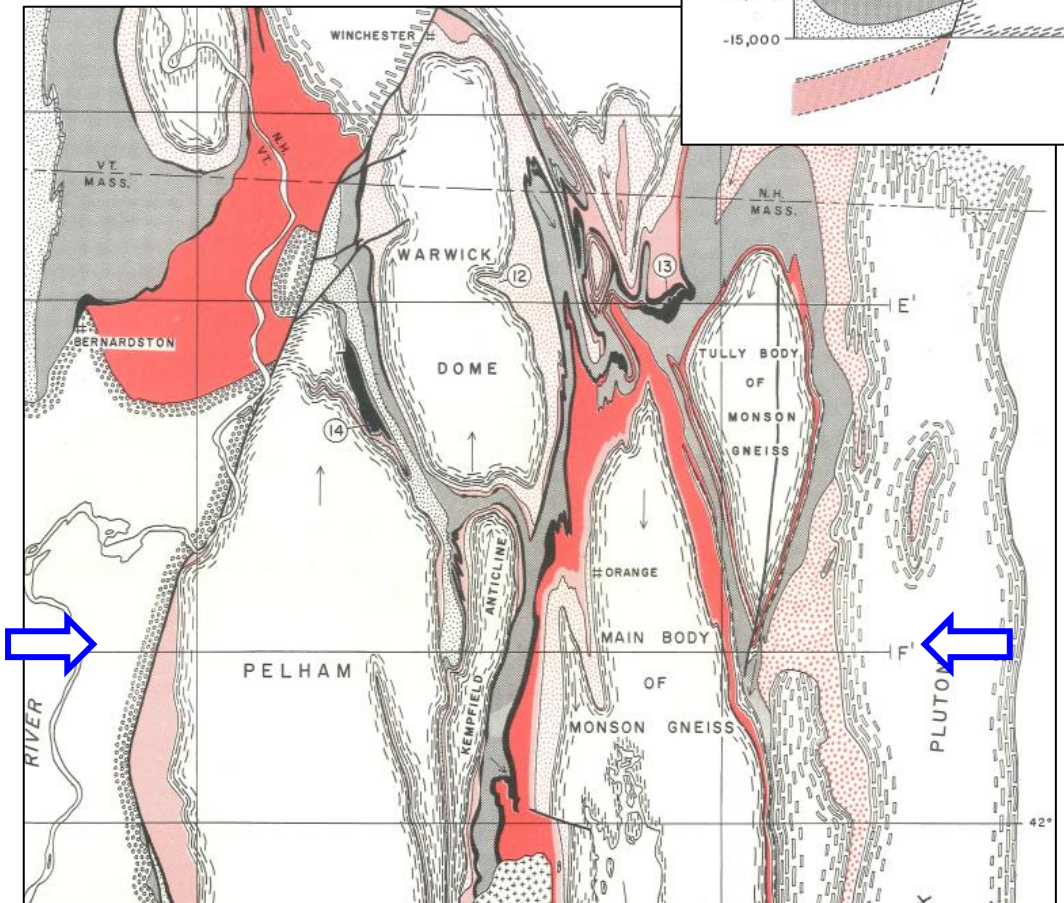

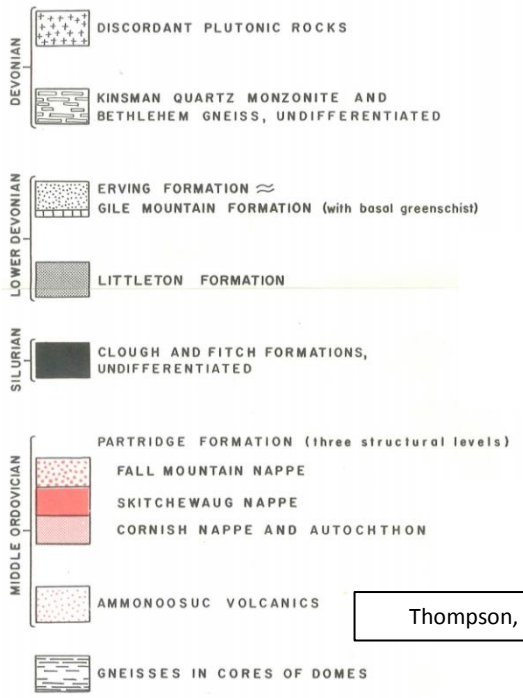

Thompson, et al., 1968

Peninsula of Tovqussaq nuna
Greenland

[Click to View Session 3.2.1 (20 MB)]

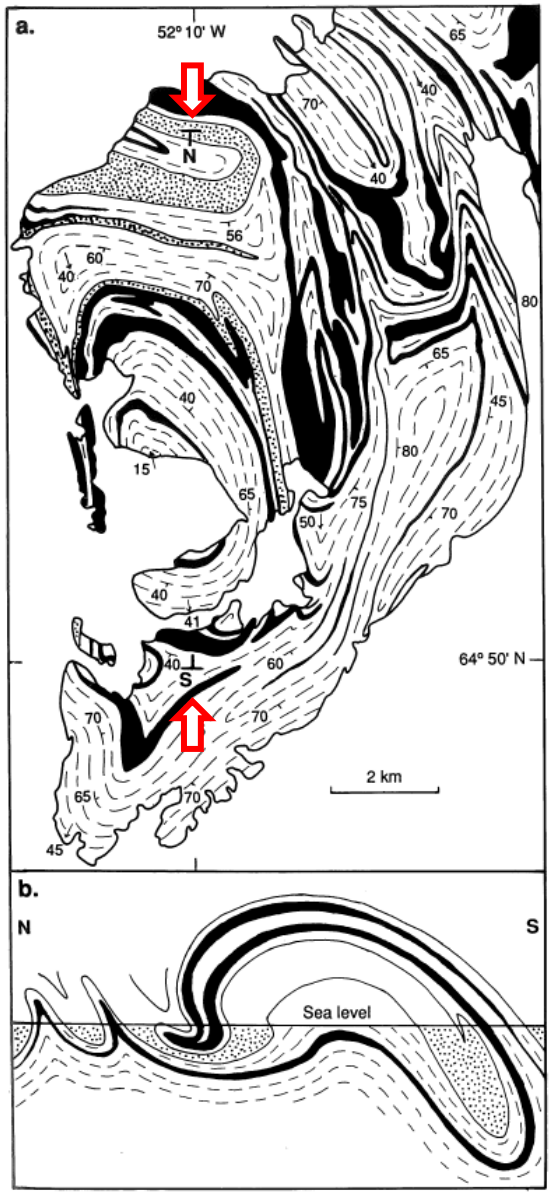

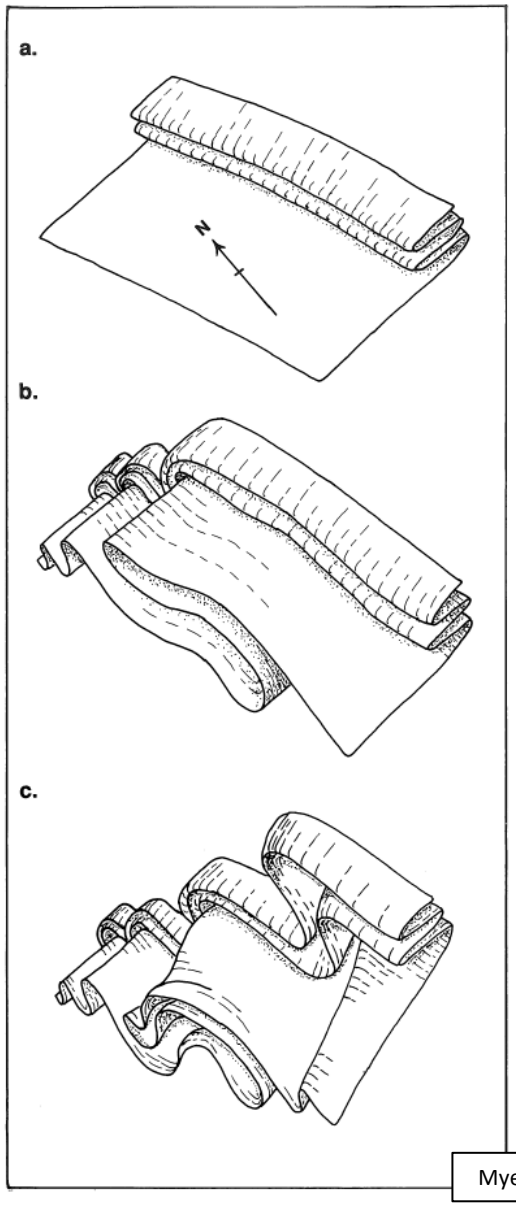

Quartzo-feldspathic gneiss
Anorthosite
Amphibolite
65 Dip and strike of layering
40 Direction and plunge of fold axis

Myers & Kroner, 1994 after Berthelsen, 1960